vessel enlargement would facilitate our understanding of the process of caliber size determination during angiogenesis.

On the other hand, VEGFs and their cognate receptors (VEGFRs), play central roles in the proliferation of ECs under physiological conditions (23); however, in contrast to Angl, transgenic overexpression of VEGF in keratinocytes induces formation of a greater number of blood vessels in the dermis, but these were reported to be exclusively of very small caliber (20).

Both VEGF and Angl are required for the process of angiogenesis. What happens when both Angl and VEGF are overexpressed? Double transgenic mice expressing both these factors in keratinocytes had blood vessels in the dermis larger than wild-type mice but smaller than mice transgenic for Angl alone (20). Therefore, the relative amounts of Angl and VEGF may alter the caliber size of blood vessels and molecules affected by VEGFR. Hence, Tie2 on ECs must be involved in the regulation of caliber size in blood vessels.

Genes upregulated following Angl binding to Tie2 on ECs have been identified by the subtraction method. In this way, the apelin gene was isolated from human umbilical venous endothelial cells (HUVECs) (24). Of many proangiogenic cytokines, such as Angl, VEGF, bFGF, PDGF-BB, and EGF, it was found that apelin expression was upregulated in HUVECs only by Angl and bFGF (Table 1).

Table 1: Apelin and APJ expression on HUVECs stimulated by angiogenic cytokines.

	Apelin	APJ
Angl	⇑	–
VEGF-A	–	⇑
bFGF	⇑	–
PDGF-BB	–	–
EGF	–	–

⇑ induced, – :not induced.

Table 2: APJ expression on endothelial cells from different tissues.

E10.5 AGM	+++
E10.5 Yolk Sac	++
E10.5 head	++
E10.5 heart	+/-
adult heart	+/-
adult liver	+/-
adult tumor	+

E10.5: embryonic day 10.5, adult: 8 weeks-old. +: positive, +/-:weak.

Apelin, a ligand for APJ, was recently isolated as a bioactive peptide from bovine gastric extract. The apelin gene encodes a protein of 77 amino acids, which can generate two active polypeptides: the long (42–77) and the short (65–77) forms of apelin (25–27), which both activate APJ. Apelin mRNA and protein are highly expressed in the lung and mammary gland. However, the distribution of the different molecular forms of apelin differs among tissues: apelin molecules with sizes close to apelin-36 (long forms) are major components in the lung, testis, and uterus, but both long and short (approximating apelin-13) forms are detected in the mammary gland (26).

APJ is a G protein-coupled receptor, reportedly expressed in the cardiovascular and central nervous systems (28, 29). In the brain, APJ expression is observed in neurons (30) as well as in oligodendrocytes and astrocytes (31). In the brain, the apelin/APJ system plays a role in maintaining body fluid homeostasis and regulating the release of vasopressin from the hypothalamus (32). In the cardiovascular system, APJ is expressed in the endothelial lineage in various species of amphibians, as well as in mice and humans (29, 33, 34). In the latter two, the expression of the receptor has also been detected by immunocytochemistry in vascular smooth muscle cells and cardiomyocytes (35). Apelin/APJ function in cardiomyocytes is thought to associate with a very strong inotropic activity (36, 37). The function of apelin/APJ in the EC lineage is reported to be associated with the hypotensive activity of apelin (38), as the activation of APJ leads to nitric oxide (NO) production by the ECs (39), and this possibly plays a role in the relaxation of the smooth muscle cell.

Using morpholino antisense oligonucleotides (MO), requisite roles of the apelin/APJ system have been reported in the cardiovascular system of *Xenopus laevis* (40, 41) and Zebrafish (42). *Xenopus apelin* (*Xapelin*) was detected in the region around the presumptive blood vessels during early embryogenesis and overlapped with the expression of *Xmsr*, the *Xenopus* homolog of *APJ*. Overexpression of *Xapelin* disorganised the expression of the endothelial precursor cell marker *XlFli* at the neurula stage. Knock down of *Xapelin or* Xmsr induced abnormal heart morphology and attenuated the expression of *Tie2*, resulting in the disruption of blood vessel formation in the posterior cardinal vein, intersomitic vessels, and vitelline vessels. In contrast, apelin protein has been shown to induce angiogenesis in the chicken chorioallantoic membrane assay (41).

APJ expression on EC lineage cells and the phenotype of apelin-deficient mice

APJ expression is observed in the EC lineage in mammals; however, when apelin first becomes expressed by ECs and which ECs express its receptor APJ is not clear. During early embryogenesis, compared to ECs from other tissues, such as yolk sac, head region, and heart at the same stage (E10.5), ECs from the the AGM region [Aorta-Gonad-Mesonephros region followed by para-aortic splanchnopleural mesoderm (P-Sp) region at embryonic day (E) 10.5 to E11.5], in which angiogenesis is actively taking place, strongly express APJ (Table 2). However, in the adult, ECs from heart and liver express it only very weakly, but ECs of blood vessels in tumors have been reported to express APJ more strongly (43).

During early embryogenesis at E8.5–9.5, APJ is expressed on ECs sprouted from the dorsal aorta. However, it is not on ECs of the dorsal aorta constructed by vasculogenesis processes. ECs sprouted from dorsal aorta form intersomitic vessels and most express APJ at E8.5; however, APJ expression is observed on ECs in the migrating tip region of intersomitic vessels at E9.5 (24). Therefore, taken together, these expression profiles suggest that APJ is expressed by ECs during angiogenesis but not vasculogenesis. In the neonate,

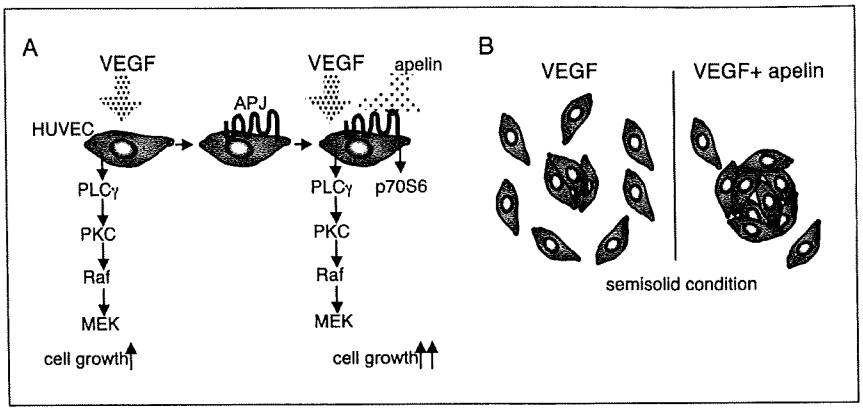

Figure 2: Effect of VEGF and apelin on proliferation and assembly of ECs. A) VEGF activates the PLCγ-PKC-Raf-1-MEK-MAP kinase pathway through its cognate receptor. VEGF also induces expression of the apelin receptor APJ on HUVECs. Apelin then activates p70S6 kinase. Therefore, VEGF and apelin coordinately enhance the proliferation of HUVECs. B) Apelin function in spheroid formation by ECs. In semisolid culture media, HUVECs pre-stimulated with VEGF generate larger spheroids in the presence of apelin than with VEGF alone.

APJ expression is observed in ECs of blood vessels in the dermis, but gradually disappears with maturity. These expression patterns strongly suggest that APJ plays a spatio-temporal role for the maturation of blood vessels by transient expression on ECs where angiogenesis is taking place. Generally, apelin-deficient mutant animals appear healthy as adults, but although body size and number of somites was similar between wild-type and apelin mutant embryos at E9.5, the caliber of intersomitic vessels was narrower in the apelin-deficient embryos (24). Moreover, the blood vessels observed in the trachea, dermis, heart and other organs were narrower than those in wild-type mice after birth. Therefore, it is suggested that apelin regulates caliber size of blood vessels.

Coordinate effect of apelin with VEGF for the proliferation of HUVECs

It is well known that VEGF induces proliferation of HUVECs. However, apelin alone is not so effective in this respect. Because APJ expression is observed in ECs during angiogenesis, it is possible that apelin cannot function in the absence of VEGF, which is upregulated during angiogenesis in response to tissue hypoxia. HUVECs do not constitutively express APJ strongly; however, it is greatly upregulated on stimulation with VEGF (Table 1). Therefore, in the presence of VEGF, HUVECs can respond to apelin effectively. Indeed, apelin alone does not affect proliferation of HUVECs, but in the presence of VEGF, it enhances their proliferation to VEGF (24).

It has been reported that VEGF-A-induced activation of the Raf-1–MEK–MAP kinase pathway mediated mainly by activation of PLCγ and subsequent stimulation of PKC (particularly PKCβ) resulted in the proliferation of ECs (44, 45). Recently, it has been reported that apelin activates p70S6 kinase for cell-cycle progression (46). Therefore, VEGF and apelin may coordinately induce proliferation of HUVECs (Fig. 2).

Alone among the proangiogenic cytokines, such as Ang1, bFGF, PDGF-BB, and EGF, VEGF induces APJ expression on HUVECs (Table 1). Of course, other molecules may also affect APJ expression on ECs; however, it is very interesting that VEGF affects APJ expression, suggesting a close relationship between the APJ/apelin system and tissue hypoxia in which angiogenesis is induced.

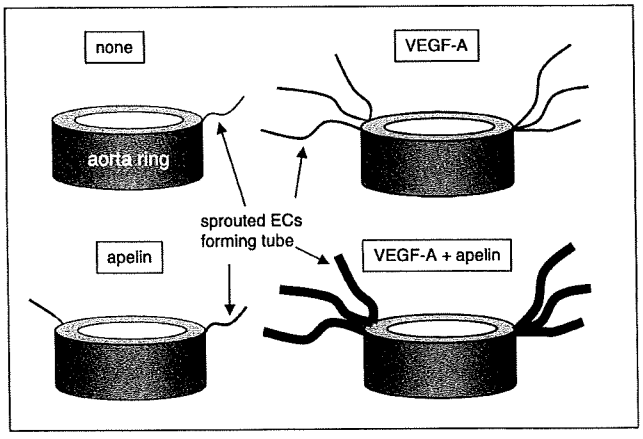

Figure 3: Apelin and VEGF together induce enlarged capillary tube formation in the aorta ring assay. Apelin alone does not induce capillary tube formation in the aorta ring assay. However, in the presence of VEGF, it induces larger capillary tubes than VEGF alone.

Apelin regulates cell assembly in spheroids

Spheroid models of cells have been widely used in tumor and embryonic stem cell studies of cellular differentiation, cell-cell interactions, and hypoxia responses, and were recently utilised to induce proliferation of neural stem cells. Based on these studies, Korff and Augustin (47) developed a spheroid culture system of ECs, such as HUVECs or bovine aortic ECs (BAECs) and showed that these three-dimensional spheroid EC models are useful for the analysis of differentiated cell function. In this culture system, ECs are suspended in culture medium containing 20% methocel, seeded into non-adhesive bacteriological dishes and cultured. Under these conditions, suspended ECs aggregate spontaneously within 4 hours to form cellular aggregates of varying size and cell number (24). Therefore, molecules affecting cell-to-cell assembly can induce larger spheroids in this culture system. When HUVECs were pretreated with VEGF for the induction of APJ and maintained in this spheroid culture system in the presence of apelin, this agent induced the formation of

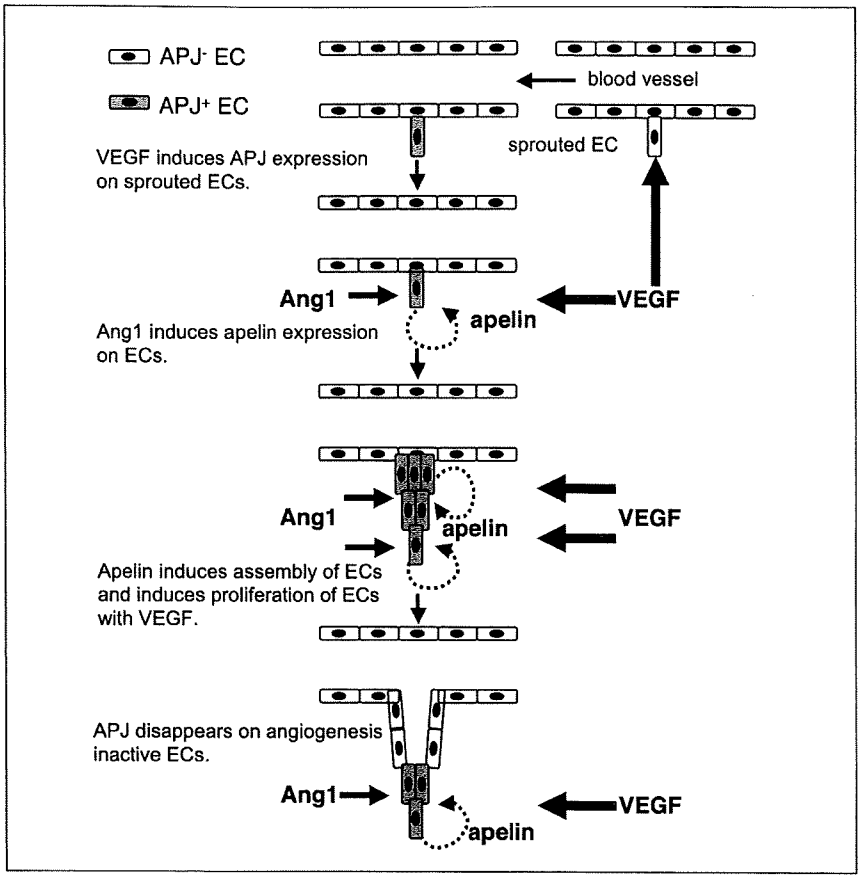

Figure 4: Apelin is involved in the regulation of blood vessel caliber size. Endothelial sprouts from pre-existing vessels express APJ following stimulation with VEGF. During angiogenesis, when the Tie2 agonist, Ang1, stimulates ECs sprouted from vessels, apelin expression is induced in these cells. VEGF and apelin coordinately enhance proliferation and assembly of ECs, resulting in the formation of larger tubes. VEGF continuously stimulates ECs during angiogenesis; however, once VEGF expression is reduced in the foci, APJ expression is down-regulated in ECs and caliber size regulation is finalised.

larger spheroids than VEGF alone (Fig. 2). Induction of APJ on Ba/F3 hematopoietic cells (pro-B lymphocyte cell line), also facilitated their aggregation upon stimulation with apelin (Kidoya and Takakura unpublished data). These data indicate that apelin acts on cell-to-cell aggregation or assembly.

When ECs are cultured on Matrigel, a solid gel of basement membrane proteins, they rapidly align and form hollow tube-like structures. Grant et al. (48) first reported this effect of Matrigel. In the original study, the authors reported that tube formation is a multi-step process induced by laminin and that laminin-derived synthetic peptides can induce single-cell hollowing. However, in a similar culture system, Kamei et al. (17) induced cord hollowing to create enlarged tubes. Therefore, this culture system can be utilised to examine whether a certain molecule regulates capillary caliber size. HUVECs cultured on Matrigels in the presence of apelin generate larger tube-like structures than when they are cultured in the presence of VEGF (24). Therefore, this indicates that apelin is involved in cord hollowing.

Apelin induces formation of large tubes in the aorta ring assay *ex vivo*

The aorta ring assay, first reported by Nicosia and Madri in 1987 (49), can be employed to explore the roles of angiogenesis-related molecules *ex vivo*. This report described the utilization of rat aorta "rings" as explants. Several subsequent studies modified this method; now most researchers culture aorta rings in a three-dimensional (3-D) extracellular matrix, such as type I collagen or Matrigel. Under these culture conditions, ring explants generate capillary-like endothelial sprouts *in vitro*. Thus, this culture system mimics sprouting angiogenesis from pre-existing blood vessels.

Upon addition of proangiogenic factors or anti-angiogenic factors, formation of capillary-like tubes is affected (Fig. 3). In the absence of growth factors, very small numbers and very short capillary-like structures are observed. However, upon addition of VEGF, capillary-like tubes radially sprout from the aorta ring. In this 3-D system, apelin alone does not induce abundant capillary-like tube formation, but in the presence of VEGF, the caliber size of the capillary tube is enlarged by apelin. In culture there is of course no blood flow through capillary-like tubes, showing that the effect of apelin on capillary enlargement is independent of blood flow.

Apelin acts as a potent caliber size regulator by inducing cord hollowing

Given the expression of APJ on ECs and the function of apelin, the role of this molecule in inducing enlarged blood vessels by promoting proliferation and cell-to-cell aggregation/assembly may be as follows (Fig. 4). Upon stimulation by VEGF, ECs

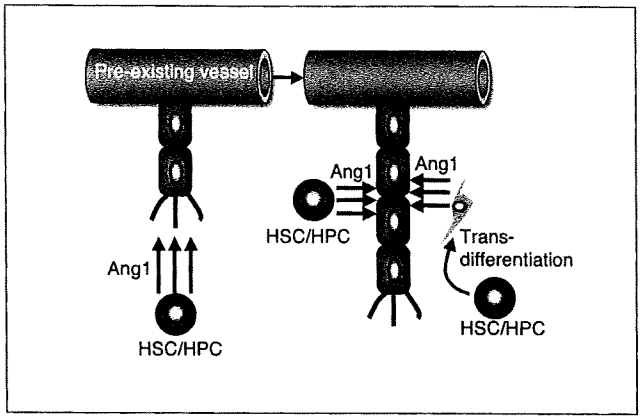

Figure 5: Function of HSCs/HPCs and production of Angl. Haematopoietic stem cells (HSCs) and progenitor cells (HPCs) migrate into avascular regions and produce Angl, which then induces chemotaxis of ECs and determines the migration direction of EC sprouting. Therefore, in this case, HSCs/HPCs act as proangiogenic accessory cell components. Moreover, HSCs/HPCs located at perivascular regions differentiate into mural-like cells. Both HSCs/HPCs and such mural-like cells produce Angl and then induce apelin expression in ECs to regulate vascular diameter.

sprouted from pre-existing vessels express APJ. Subsequently, Angl or bFGF stimulates such sprouted ECs to express apelin. In the presence of both VEGF and apelin, EC proliferation is enhanced more than in the presence of VEGF alone. They then adhere and form contacts with each other through junctional proteins, and construct enlarged blood vessels. Upon stimulation of APJ by apelin, junctional proteins such as Claudin-5 and VE-Cadherin are upregulated in HUVECs (24). When VEGF ceases to affect ECs, APJ expression is lost, and the modification of caliber size is finalised. As described above (Fig. 1), the single-cell hollowing system generates narrow capillaries and the cord hollowing system is responsible for the production of larger blood vessels. Therefore, apelin may function in the later, cord hollowing system and be involved in the size determination of blood vessels during angiogenesis.

Haematopoietic stem cells are candidate sources of Angl for the production of apelin during angiogenesis

Angl is usually produced from MCs in cells composing blood vessels (50). However, haematopoietic stem cells (HSCs) and progenitor cells (HPCs) also produce Angl (51). HSCs/HPCs migrate into avascular areas before ECs, so Angl from these cells can induce angiogenesis by promoting EC chemotaxis (51). Moreover, HSCs/HPCs induce the enlargement of blood vessels observed in the fibrous cap surrounding tumors (52) and Angl from HSCs/HPCs in embryos, as well as adults, facilitates structural stability of newlydeveloped blood vessels as a physiological function during angiogenesis (53). Indeed, AML1/RUNX1 mutant embryos that lack HSCs have unstable blood vessels which frequently rupture (53–55). These findings support the notion that HSCs play an important role in structural stabilization of blood vessels. HSCs/HPCs are suggested to give rise to MCs (53, 56), which are a major source of Angl. Therefore, it is possible that Angl from the HSC/HPC population, frequently observed in ischemic regions, and from MCs differentiated from HSCs/HPCs, is the source of Tie2 activation during angiogenesis (Fig. 5). Angl produced in this manner then induces the production of apelin from ECs.

Conclusions

Control of blood vessel caliber changes is an important mechanism influencing blood pressure and flow, especially for larger vessels, and is a fundamental event for supplying oxygen and nutrients in smaller vessels. The apelin/APJ system may be involved in the size-sensing mechanism of blood vessels. Knockingout the apelin gene suggests that molecular cues other than apelin can rescue narrow caliber size blood vessels by compensational upregulation, because in the early stage of embryogenesis the narrow caliber of intersomitic vessels, observed in apelin mutant embryos, was rescued in the later stage (24). To further clarify the size-sensing mechanism of blood vessels, isolation of upregulated molecules responsible for such compensation of blood vessel caliber in apelin mutant embryos will be required.

Recently, therapeutic angiogenesis using genes or cytokines such as VEGF, HGF, etc. and cells from bone marrow or peripheral blood has been applied to the clinical management of ischemic patients (57). For the development of ideal therapeutic angiogenesis modulators, molecules controlling the caliber size of newly developing blood vessel would be the preferred choice. Apelin could be one candidate for such a modulator.

References

1. Risau W. Mechanisms of angiogenesis. Nature 1997; 386: 671–674.
2. Gale NW, Yancopoulos GD. Growth factors acting via endothelial cell-specific receptor tyrosine kinases: VEGFs, angiopoietins, and ephrins in vascular development. Genes Dev 1999; 13: 1055–1066.
3. Oettgen P. Transcriptional regulation of vascular development. Circ Res 2001; 89: 380–383.
4. Carmeliet P. Angiogenesis in health and disease. Nat Med 2003; 9: 653–660.
5. Gerhardt H, Betsholtz C. Endothelial-pericyte interactions in angiogenesis. Cell Tissue Res 2003; 314: 15–23.
6. Simon MC. Vascular morphogenesis and the formation of vascular networks. Dev Cell 2004; 6: 479–482.
7. Wang HU, Chen ZF, Anderson DJ. Molecular distinction and angiogenic interaction between embryonic arteries and veins revealed by ephrin-B2 and its receptor Eph-B4. Cell 1998; 93: 741–753.
8. Adams RH, Wilkinson GA, Weiss C, et al. Roles of ephrinB ligands and EphB receptors in cardiovascular development: demarcation of arterial/venous domains, vascular morphogenesis, and sprouting angiogenesis. Genes Dev 1999; 13: 295–306.
9. Zhong TP, Childs S, Leu JP, et al. Gridlock signalling pathway fashions the first embryonic artery. Nature 2001; 414: 216–220.
10. Morawietz H, Breier G. Endothelial cell biology: an update. 5th International Symposium on the Biology

of Endothelial Cells. Thromb Haemost 2006; 95: 1025–1030.
11. Lindahl P, Johansson BR, Leveen P, et al. Pericyte loss and microaneurysm formation in PDGF-B-deficient mice. Science 1997; 277: 242–245.
12. Dumont DJ, Gradwohl G, Fong GH, et al. Dominant-negative and targeted null mutations in the endothelial receptor tyrosine kinase, tek, reveal a critical role in vasculogenesis of the embryo. Genes Dev 1994; 8: 1897–1909.
13. Sato TN, Tozawa Y, Deutsch U, et al. Distinct roles of the receptor tyrosine kinases Tie-1 and Tie-2 in blood vessel formation. Nature 1995; 376: 70–74.
14. Suri C, Jones PF, Patan S, et al. Requisite role of angiopoietin-1, a ligand for the TIE2 receptor, during embryonic angiogenesis. Cell 1996; 87: 1171–1180.
15. Feng Y, vom Hagen F, Pfister F, et al. Impaired pericyte recruitment and abnormal retinal angiogenesis as a result of angiopoietin-2 overexpression. Thromb Haemost 2007; 97: 99–108.
16. Lubarsky B, Krasnow MA. Tube morphogenesis: making and shaping biological tubes. Cell 2003; 112: 19–28.
17. Kamei M, Saunders WB, Bayless KJ, et al. Endothelial tubes assemble from intracellular vacuoles in vivo. Nature 2006; 442: 453–456.
18. Folkman J, Haudenschild C. Angiogenesis in vitro. Nature 1980; 288: 551–556.
19. Parker LH, Schmidt M, Jin SW, et al. The endothelial-cell-derived secreted factor Egfl7 regulates vascular tube formation. Nature 2004; 428: 754–758.
20. Suri C, McClain J, Thurston G, et al. Increased vascularization in mice overexpressing angiopoietin-1. Science 1998; 282: 468–471.
21. Cho CH, Kim KE, Byun J, et al. Long-term and sustained COMP-Ang1 induces long-lasting vascular enlargement and enhanced blood flow. Circ Res 2005; 97: 86–94.
22. Thurston G, Wang Q, Baffert F, et al. Angiopoietin 1 causes vessel enlargement, without angiogenic sprouting, during a critical developmental period. Development 2005; 132: 3317–3326.
23. Ferrara N, Gerber HP, LeCouter J. The biology of VEGF and its receptors. Nat Med 2003; 9: 669–676.
24. Kidoya H, Ueno M, Yamada Y, et al. Spatial and temporal role of the apelin/APJ system in the caliber size regulation of blood vessels during angiogenesis. EMBO J 2008; 27: 522–534.
25. Tatemoto K, Hosoya M, Habata Y, et al. Isolation and characterization of a novel endogenous peptide ligand for the human APJ receptor. Biochem Biophys Res Commun 1998; 251: 471–476.
26. Kawamata Y, Habata Y, Fukusumi S, et al. Molecular properties of apelin: tissue distribution and receptor binding. Biochim Biophys Acta 2001; 1538: 162–171.
27. Masri B, Knibiehler B, Audigier Y. Apelin signalling: a promising pathway from cloning to pharmacology. Cell Signal 2005; 17: 415–426.
28. O'Dowd BF, Heiber M, Chan A, et al. A human gene that shows identity with the gene encoding the angiotensin receptor is located on chromosome 11. Gene 1993; 136: 355–360.
29. Devic E, Rizzoti K, Bodin S, et al. Amino acid sequence and embryonic expression of msr/apj, the mouse homolog of Xenopus X-msr and human APJ. Mech Dev 1999; 84: 199–203.
30. Edinger AL, Hoffman TL, Sharron M, et al. An orphan seven-transmembrane domain receptor expressed widely in the brain functions as a coreceptor for human immunodeficiency virus type 1 and simian immunodeficiency virus. J Virol 1998; 72: 7934–7940.
31. Croitoru-Lamoury J, Guillemin GJ, Boussin FD, et al. Expression of chemokines and their receptors in human and simian astrocytes: evidence for a central role of TNF alpha and IFN gamma in CXCR4 and CCR5 modulation. Glia 2003; 41: 354–370.
32. De Mota N, Reaux-Le Goazigo A, El Messari S, et al. Apelin, a potent diuretic neuropeptide counteracting vasopressin actions through inhibition of vasopressin neuron activity and vasopressin release. Proc Natl Acad Sci USA 2004; 101: 10464–10469.
33. Devic E, Paquereau L, Vernier P, et al. Expression of a new G protein-coupled receptor X-msr is associated with an endothelial lineage in Xenopus laevis. Mech Dev 1996; 59: 129–140.
34. Katugampola SD, Maguire JJ, Matthewson SR, et al. [(125)I]-(Pyr(1))Apelin-13 is a novel radioligand for localizing the APJ orphan receptor in human and rat tissues with evidence for a vasoconstrictor role in man. Br J Pharmacol 2001; 132: 1255–1260.
35. Kleinz MJ, Davenport AP. Immunocytochemical localization of the endogenous vasoactive peptide apelin to human vascular and endocardial endothelial cells. Regul Pept 2004; 118: 119–125.
36. Szokodi I, Tavi P, Foldes G, et al. Apelin, the novel endogenous ligand of the orphan receptor APJ, regulates cardiac contractility. Circ Res 2002; 91: 434–440.
37. Ashley EA, Powers J, Chen M, et al. The endogenous peptide apelin potently improves cardiac contractility and reduces cardiac loading in vivo. Cardiovasc Res 2005; 65: 73–82.
38. Ishida J, Hashimoto T, Hashimoto Y, et al. Regulatory roles for APJ, a seven-transmembrane receptor related to angiotensin-type 1 receptor in blood pressure in vivo. J Biol Chem 2004; 279: 26274–26279.
39. Tatemoto K, Takayama K, Zou MX, et al. The novel peptide apelin lowers blood pressure via a nitric oxide-dependent mechanism. Regul Pept 2001; 99: 87–92.
40. Inui M, Fukui A, Ito Y, et al. Xapelin and Xmsr are required for cardiovascular development in Xenopus laevis. Dev Biol 2006; 298: 188–200.
41. Cox CM, D'Agostino SL, Miller MK, et al. Apelin, the ligand for the endothelial G-protein-coupled receptor, APJ, is a potent angiogenic factor required for normal vascular development of the frog embryo. Dev Biol 2006; 296: 177–189.
42. Scott IC, Masri B, D'Amico LA, et al. The g protein-coupled receptor agtrl1b regulates early development of myocardial progenitors. Dev Cell 2007; 12: 403–413.
43. Kalin RE, Kretz MP, Meyer AM, et al. Paracrine and autocrine mechanisms of apelin signaling govern embryonic and tumor angiogenesis. Dev Biol 2007; 305: 599–614.
44. Takahashi T, Yamaguchi S, Chida K, et al. A single autophosphorylation site on KDR/Flk-1 is essential for VEGF-A-dependent activation of PLC-gamma and DNA synthesis in vascular endothelial cells. EMBO J 2001; 20: 2768–2778.
45. Hofer E, Schweighofer B. Signal transduction induced in endothelial cells by growth factor receptors involved in angiogenesis. Thromb Haemost 2007; 97: 355–363.
46. Masri B, Morin N, Cornu M, et al. Apelin (65–77) activates p70 S6 kinase and is mitogenic for umbilical endothelial cells. FASEB J 2004; 18: 1909–1911.
47. Korff T, Augustin HG. Integration of endothelial cells in multicellular spheroids prevents apoptosis and induces differentiation. J Cell Biol 1998; 143: 1341–1352.
48. Grant DS, Lelkes PI, Fukuda K, et al. Intracellular mechanisms involved in basement membrane induced blood vessel differentiation in vitro. In Vitro Cell Dev Biol 1991; 27: 327–336.
49. Nicosia RF, Madri JA. The microvascular extracellular matrix. Developmental changes during angiogenesis in the aortic ring-plasma clot model. Am J Pathol 1987; 128: 78–90.
50. Davis S, Aldrich TH, Jones PF, et al. Isolation of angiopoietin-1, a ligand for the TIE2 receptor, by secretion-trap expression cloning. Cell 1996; 87: 1161–1169.
51. Takakura N, Watanabe T, Suenobu S, et al. A role for hematopoietic stem cells in promoting angiogenesis. Cell 2000; 102: 199–209.
52. Okamoto R, Ueno M, Yamada Y, et al. Hematopoietic cells regulate the angiogenic switch during tumorigenesis. Blood 2005; 105: 2757–2763.
53. Yamada Y, Takakura N. Physiological pathway of differentiation of hematopoietic stem cell population into mural cells. J Exp Med 2006; 203:1055–1065.
54. Okuda T, van Deursen J, Hiebert SW, et al. AML1, the target of multiple chromosomal translocations in human leukemia, is essential for normal fetal liver hematopoiesis. Cell 1996; 84: 321–330.
55. Okada H, Watanabe T, Niki M, et al. AML1(-/-) embryos do not express certain hematopoiesis-related gene transcripts including those of the PU.1 gene. Oncogene 1998; 17: 2287–2293.
56. Sata M, Saiura A, Kunisato A, et al. Hematopoietic stem cells differentiate into vascular cells that participate in the pathogenesis of atherosclerosis. Nat Med 2002; 8: 403–409.
57. Huang PP, Yang XF, Li SZ, et al. Randomised comparison of G-CSF-mobilized peripheral blood mononuclear cells versus bone marrow-mononuclear cells for the treatment of patients with lower limb arteriosclerosis obliterans. Thromb Haemost 2007; 98: 1335–1342.

EXPERIMENTAL CELL RESEARCH 315 (2009) 2818–2823

available at www.sciencedirect.com

ScienceDirect

www.elsevier.com/locate/yexcr

ELSEVIER

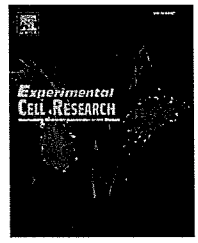

Research Article

Lipid rafts serve as signaling platforms for Tie2 receptor tyrosine kinase in vascular endothelial cells

*Shin-Ya Katoh, Takahiro Kamimoto, Daishi Yamakawa, Nobuyuki Takakura**

Department of Signal Transduction, Research Institute for Microbial Diseases, Osaka University, 3-1 Yamada-oka, Suita, Osaka 565-0871, Japan

ARTICLE INFORMATION

Article Chronology:
Received 13 January 2009
Revised version received 3 July 2009
Accepted 8 July 2009
Available online 15 July 2009

Keywords:
Tie2
Angiopoietin-1
Lipid rafts
Akt
Erk
FoxO

ABSTRACT

The Tie2 receptor tyrosine kinase plays a pivotal role in vascular and hematopoietic development. The major intracellular signaling systems activated by Tie2 in response to Angiopoietin-1 (Ang1) include the Akt and Erk1/2 pathways. Here, we investigated the role of cholesterol-rich plasma membrane microdomains (lipid rafts) in Tie2 regulation. Tie2 could not be detected in the lipid raft fraction of human umbilical vein endothelial cells (HUVECs) unless they were first stimulated with Ang1. After stimulation, a minor fraction of Tie2 associated tightly with the lipid rafts. Treatment of HUVECs with the lipid raft disrupting agent methyl-β-cyclodextrin selectively inhibited Ang1-induced Akt phosphorylation, but not Erk1/2 phosphorylation. It has been reported that inhibition of FoxO activity is an important mechanism for Ang1-stimulated Tie2-mediated endothelial function. Consistent with this, we found that phosphorylation of FoxO mediated by Tie2 activation was attenuated by lipid raft disruption. Therefore, we propose that lipid rafts serve as signaling platforms for Tie2 receptor tyrosine kinase in vascular endothelial cells, especially for the Akt pathway.

Introduction

Angiogenesis, the outgrowth of novel blood vessels from pre-existing ones, is essential for a number of physiological processes such as embryonic development, organ formation, tissue regeneration, and tissue remodeling [1]. However, under pathological conditions, uncontrolled angiogenesis sustains the progression of many diseases, including diabetic retinopathy, psoriasis, rheumatoid arthritis, and tumor growth [1]. In the latter condition, numerous studies have provided evidence that tumor growth and metastasis are angiogenesis dependent [2]. Therefore, it is necessary to analyze the molecular mechanism of angiogenesis to develop angiogenesis disrupting agents.

Angiopoietin-1 (Ang1) is the ligand of the endothelial tyrosine kinase receptor Tie2 [3]. Mice lacking Ang1 die during embryogenesis (E12.5) showing a poorly remodeled and immature vasculature with defects in endothelial cell (EC) adhesion to mural cells [4]. Ang1 is a potent and unique angiogenic protein that induces EC migration and survival. The Ang1-Tie2 system seems to have different functions for blood vessels depending on the situation of ECs. Recently, it has been suggested that Tie2 activation by Ang1 induces phosphorylation of Akt rather than Erk when EC–EC contact is established, resulting in quiescence of blood vessel formation [5]. On the other hand, when ECs are migrating and proliferating, Tie2 mainly activates the Erk pathway rather than Akt, resulting in progression of angiogenesis. Therefore, utilization of the Akt or Erk pathway is key for explaining the different functions of Tie2 in blood vessel formation. However, how such signaling diversity occurs by a single Tie2 receptor is not fully elucidated.

Plasma membrane lipid raft domains, which contain high concentrations of cholesterol and sphingolipids [6,7], are known to function as centers for the assembly of signaling complexes. Such assembly is suggested to facilitate both specificity and the rate of signaling events, and they have become a central facet of signaling research since the function of many receptors and their

* *Corresponding author.* Fax: +81 6 6879 8314.
E-mail address: ntakaku@biken.osaka-u.ac.jp (N. Takakura).

0014-4827/$ – see front matter © 2009 Elsevier Inc. All rights reserved.
doi:10.1016/j.yexcr.2009.07.008

downstream effectors are dependent on lipid rafts [8–11]. The presence of receptor and effector proteins in lipid rafts, as well as the ability of lipid rafts to enhance receptor signaling [12], has led to the concept of a signalosome where proteins are localized together to facilitate receptor signaling following agonist exposure [8,13]. For some receptors, lipid raft complexes appear to play an inhibitory role [12], although this need not conflict with signal facilitation if inhibition is directed at the unstimulated receptor.

Here, we hypothesize that Ang1-Tie2 could mediate different biologic effects under the influence of lipid rafts. We show here that lipid rafts are essential components for Tie2-Akt pathway activation, but not Tie2-Erk pathway activation. These data suggest that lipid rafts serve as signaling platforms for the Tie2 receptor tyrosine kinase and could mediate different biologic effects in vascular ECs.

Materials and methods

Reagents and antibodies

Recombinant human angiopoietin-1 (Ang1) was purchased from R&D systems (Minneapolis, MN). Monoclonal anti-caveolin-1 antibody was purchased from BD Transduction Laboratories (Lexington, KY). Monoclonal anti-Tie2 antibody was purchased from Upstate (Lake Placid, NY). Monoclonal anti-transferrin receptor antibody was purchased from Zymed (South San Francisco, CA). Monoclonal anti-GAPDH antibody was purchased from Chemicon (Temecula, CA). Monoclonal anti-Na^+/K^+ ATPase beta 1 subunit antibody was purchased from NOVUS Biologicals (Littleton, CO). Polyclonal anti-Akt, anti-phospho-Akt (Ser473), anti-Erk1/2, anti-phospho-Erk1/2 (Thr202/Tyr204), anti-FoxO1, anti-phospho-FoxO1 (Thr24), anti-phospho-FoxO1 (Ser256), anti-phospho-FoxO1 (Ser319), anti-FoxO3a, anti-phospho-FoxO3a (Ser253), and anti-phospho-FoxO3a (Ser318/321) antibodies were purchased from Cell Signaling Technology (Beverly, MA). Polyclonal anti-phospho-Tie2 (Tyr992) antibody was purchased from R&D systems. Horseradish peroxidase (HRP)-coupled anti-mouse and anti-rabbit Ig were purchased from Jackson ImmunoResearch Laboratory (West Grove, PA). Alexa Fluor 488-coupled anti-rabbit IgG was purchased from Molecular Probes (Eugene, OR).

Cell culture

Human umbilical vein ECs (HUVECs) were purchased from Kurabo (Kurashiki, Japan) and maintained per manufacturer's instructions. For Ang1 stimulations, cells were starved in RPMI1640 medium containing 0.1% bovine serum albumin (BSA; Sigma, St Louis, Missouri) for 3 h in parallel with untreated cells and then stimulated with Ang1 as indicated in the figure legend. For methyl-beta-cyclodextrin (mβCD; Sigma) treatment, mβCD was added to the culture media and incubated at 37 °C as indicated in the figure legend before Ang1 was added to conditioned media.

Lipid raft isolation

Lipid rafts were isolated by two different methods. First, Opti-Prep gradient centrifugation using the 1% Triton X-100 method was performed using a previously described protocol with some modifications [14,15]. HUVECs grown to confluence in 10 cm dishes were used. After washing with PBS, cells were scraped and precipitated by centrifugation. Precipitate was lysed in 140 μL lysis buffer (25 mM Tris–HCl pH 7.4, 125 mM NaCl, 12.5 mM EDTA, 1% Triton X-100) for 30 min on ice. The lysate was added to four volumes of 50% Opti-Prep in the same lysis buffer and placed at the bottom of an ultracentrifuge tube. A 0–40% discontinuous Opti-Prep gradient was formed above the sample (0.3 mL lysis buffer without Opti-Prep, 1 mL 30% Opti prep in lysis buffer) and centrifuged at 55,000 rpm for 2 h in a TLS-55 rotor (Beckman Instruments, Fullerton, CA). Ten 0.2 mL fractions were gently collected from the top of the gradient. Second, centrifugation with 1% Triton X-100 was performed using a previously described protocol with modifications [16]. All steps were performed in a 4 °C cold room and on ice. Briefly, HUVECs grown in a six-well plate were lysed with 0.5 mL of lysis buffer (25 mM Tris–HCl pH 7.4, 125 mM NaCl, 12.5 mM EDTA, 1% Triton X-100), collected in plastic tube, and lysed on ice for 30 min. Lysate and insoluble material were centrifuged for 30 min in a microfuge at 12,000 ×g at 4 °C. The supernatant was collected (soluble fraction). Buffer was again added to the pellet and centrifuged for 10 min in a microfuge at 12,000 ×g at 4 °C. The supernatant was discarded. The pellet was solubilized in 0.1 mL of RIPA buffer (10 mM Tris–HCl pH 7.4, 1% NP-40, 0.1% sodium deoxycholate, 0.1% sodium dodecyl sulfate (SDS), 0.15 M NaCl, 1 mM EDTA-2Na).

Immuno-blotting

The proteins were separated by electrophoresis on 7.5% or 10% polyacrylamide gels containing SDS. The proteins were transferred by electroblotting to polyvinylidene difluoride membranes, and the membranes were subsequently incubated with the primary antibody. Proteins were detected with HRP-coupled secondary antibodies after extensive washing using ECL reagents (Amersham Biosciences, Piscataway, NJ) according to the manufacturer's instructions. Caveolin-1 was used as a marker for the lipid raft fraction. The Na^+/K^+ ATPase beta 1 subunit and transferrin receptor were used as markers for the non-raft fraction. GAPDH was used as an internal control. Representative data from more than three independent experiments is shown.

Immunocytochemistry

HUVECs were fixed with 4% paraformaldehyde in PBS and permeabilized with methanol. Next, the cells were incubated with anti-FoxO1 antibody, then with Alexa Fluor 488-coupled anti-rabbit IgG, and examined by fluorescence microscopy.

Statistical analysis

Results were expressed as the mean ± standard deviation (SD). Student's *t*-test was used for statistical analysis. Differences were considered statistically significant if the *P*-value was less than 0.05.

Results

Localization of Tie2 in lipid rafts

One line of research suggests that Tie2 localizes to the caveolae, a subset of lipid rafts, of ECs [17]. However, how localization of Tie2 is affected in the presence or absence of Ang1 has not been

investigated. Therefore, we analyzed the precise location of Tie2 on ECs and determined whether it is affected by Ang1 stimulation. We examined the subcellular localization of Tie2 using the gradient centrifugation method with 1% Triton X-100, the most popular method for identifying lipid raft-associated proteins [14]. As shown in Fig. 1A, most Tie2 was detected in the non-lipid raft fraction with very little in the lipid raft fraction in the absence of Ang1 stimulation. However, treatment with Ang1 resulted in an increase of Tie2 in the lipid raft fraction (although not in very large amounts). Localization of Tie2 into the raft fraction following Ang1 stimulation was prevented by mβCD treatment (Fig. 1B), suggesting that Tie2–raft interaction is induced by the binding of Ang1 to Tie2.

Akt and Erk pathway regulation by Tie2

As reported above, we found that a minor fraction of Tie2 tightly associates with lipid rafts after stimulation with Ang1. Next, we examined whether phosphorylated Tie2 is found in lipid rafts. As was shown in Fig. 1, the amount of Tie2 localizing to lipid rafts is low. This made it impossible to detect phosphorylated Tie2 in the lipid rafts following their isolation using the gradient centrifugation method with 1% Triton X-100 (data not shown). Therefore, we used an alternative method for the isolation of insoluble proteins in cold non-ionic detergents [16]. As shown in Fig. 1, Tie2 is almost undetectable in the insoluble fraction (lipid raft fraction) before Ang1 stimulation. However, Tie2 became detectable in lipid rafts from 15 to 60 min after stimulation with Ang1, peaked and decreased again by 120 min (Figs. 2A, B). On the other hand, we found Tie2 in the soluble fraction before stimulation with Ang1, the amount of which was largely unaffected by Ang1, except at 120 min (Figs. 2A, B). This attenuation of Tie2 in the soluble

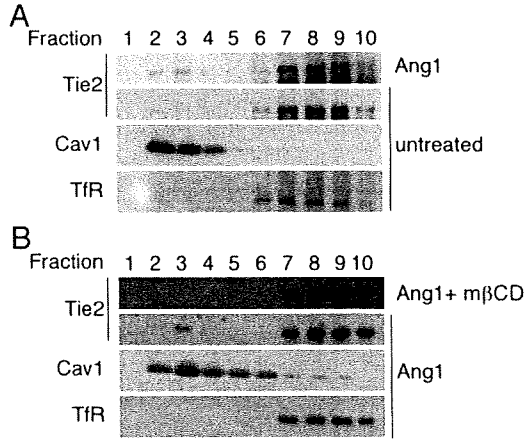

Fig. 1 – Ang1 stimulation induces localization of Tie2 in lipid rafts. (A) HUVECs were incubated with (Ang1) or without (untreated) Ang1 (200 ng/mL) for 30 min. (B) HUVECs were incubated with (Ang1 + mβCD) or without (Ang1) mβCD (10 mM) for 30 min and then incubated with Ang1 (200 ng/mL) for 30 min. In all experiments, HUVECs were fractionated by Opti-Prep gradient centrifugations with 1% Triton X-100. Fractions were collected and subjected to immuno-blotting with antibodies directed against Tie2, caveolin-1 (Cav1), or transferrin receptor (TfR). Cav1 and TfR were used as markers for lipid raft and non-raft-membrane fractions, respectively.

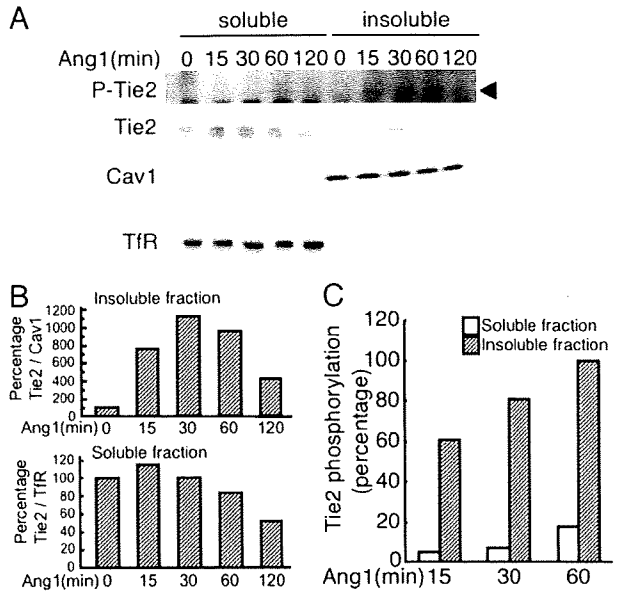

Fig. 2 – Phospho-Tie2 tightly interacts with lipid rafts. (A) HUVECs were incubated with Ang1 (200 ng/mL) for several minutes as indicated. Total cell lysates were fractionated into 1% Triton X-100 insoluble and soluble fractions. Each fraction was subjected to immuno-blotting with antibodies directed against Tie2, phospho-Tie2 (P-Tie2), caveolin-1 (Cav1), or transferrin receptor (TfR). Cav1 and TfR were as markers used for lipid raft and non-raft-membrane fractions, respectively. (B) Tie2 and Cav1, and TfR observed in (A) were quantified. The amount of Tie2 is expressed as the ratio of Tie2 to TfR or Cav1 compared to the value obtained for Ang1 untreated cells in the soluble or insoluble fractions, respectively. (C) Tie2 and P-Tie2 observed in (A) were quantified. Tie2 phosphorylation represents the ratio of phosphorylated Tie2 to total Tie2 normalized to the value obtained for the insoluble fraction stimulated for 60 min.

fraction might be caused by its down modulation at a later time point after stimulation. Tie2 phosphorylation in lipid rafts was strongly induced 30–60 min after Ang1 stimulation and subsequently decreased again (Fig. 2A). Taking account of the low amount of Tie2 protein in the insoluble compared to the soluble fraction, it appears that phospho-Tie2 tightly interacts with EC lipid rafts (Figs. 2A, C).

Next, we examined whether Tie2 expression on ECs is affected by the presence or absence of lipid rafts. As shown in Figs. 3A and B, lipid rafts disrupted by mβCD reduced the amount of Tie2 in HUVECs weakly. The difference is significant but not large. This suggested that Ang1 stimulation on ECs induces Tie2 activation even in the presence of mβCD. Indeed, treatment of HUVECs with mβCD did not inhibit Ang1-induced Tie2 phosphorylation (Fig. 3C).

Next, we examined whether disruption of lipid raft formation affects Tie2 downstream signaling. Both Akt and Erk were phosphorylated upon Ang1 treatment in the absence of mβCD (Fig. 3D). Interestingly, treatment of HUVECs with mβCD selectively inhibited Ang1-induced Akt phosphorylation but not Erk1/2 phosphorylation (Fig. 3D). In the Tie2 signaling

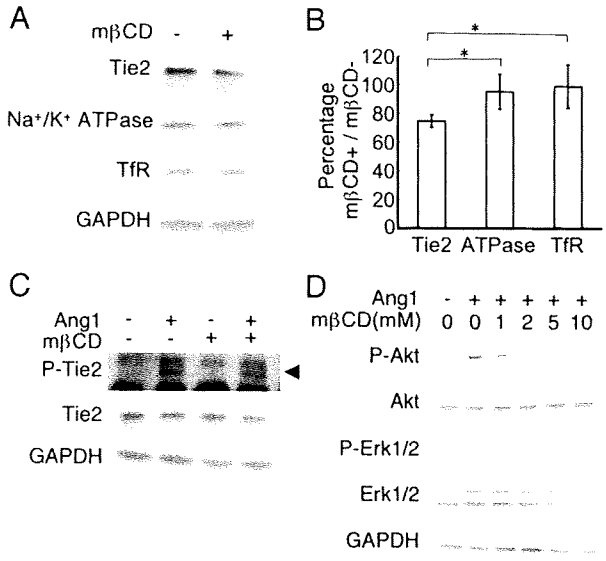

Fig. 3 – Lipid rafts serve as a signaling platform for the Tie2-Akt pathway. (A) HUVECs were incubated with or without mβCD (5 mM) for 3 h, and total protein was subjected to immuno-blotting with the indicated antibodies. (B) Tie2, Na^+/K^+ ATPase, and transferrin receptor (TfR) observed in (A) were quantified. All data were normalized to the GAPDH density and the ratio of mβCD-treated data to untreated data is presented as a percentage. ($n>3$), $^*P<0.05$. (C) HUVECs were incubated with or without mβCD (10 mM) for 15 min after serum starvation and then cultured in the presence or absence of Ang1 (200 ng/mL) for 15 min. (D) HUVECs were incubated with or without mβCD (1–10 mM) for 15 min after serum starvation and then stimulated with Ang1 (200 ng/mL) for 15 min. Total protein was subjected to immuno-blotting with the indicated antibodies.

pathway, Akt and Erk are suggested to be important for cell survival [18] and for cell migration and proliferation [19, 20], respectively. Therefore, our data suggest that lipid rafts may serve as a signaling platform for Tie2 in ECs, especially for the Akt pathway.

Activation and subcellular localization of FoxO are affected by disruption of lipid rafts

Recently, the forkhead box-containing O subfamily (FoxO), comprised of members such as FoxO1 and FoxO3a, has been reported to be important for negatively regulating vessel formation [21]. Further, inhibition of FoxO1 activity has been shown to be an important mechanism for Ang1-Tie2 mediated endothelial function [22]. It has been reported that FoxO is phosphorylated by Akt, inducing exclusion of FoxO from the nucleus and resulting in prevention of transcriptional regulation by FoxO [19,20,23–26]. Thus, we examined whether disruption of lipid rafts affects FoxO phosphorylation as mediated by Ang1 stimulation of Tie2 on HUVECs. As shown in Fig. 4A, Ang1 induced phosphorylation of FoxO1 and FoxO3a, and phosphorylation of FoxO1 and FoxO3a was attenuated by mβCD treatment. Furthermore, nuclear export of FoxO1 by Ang1 was suppressed by mβCD treatment (Figs. 4B and C). These findings indicate that lipid raft disruption inhibits FoxO inactivation in relation to Tie2 activation.

Discussion

Regulation of the Tie2 receptor has been suggested to be one way of inhibiting angiogenesis in a variety of diseases. However, it is still controversial as to whether Ang1 is a proangiogenic or anti-angiogenic factor. Within the Tie2-mediated signaling pathway, Akt and Erk have been suggested to be important regulators of angiogenesis [27,28]. Due to the diverse signaling network downstream of Akt and differences observed in short-term versus long-term Akt activation, its role in pathophysiological processes remains elusive. For example, whereas short-term Akt activation in the heart resulted in increased angiogenesis, chronic activation led to decreased angiogenesis and increased fibrosis [29,30]. In terms of the Tie2 signaling pathway, activation of Akt through Tie2 activation induces cell survival [18]. Therefore, this pathway is thought to contribute to the maintenance of vascular quiescence or stability. In contrast to this Akt pathway, activation of Erk is suggested to be important for cell migration and proliferation [19,20]. Recently, it has been reported that Tie2 activation at cell–cell or cell–substratum contacts leads to preferential activation of Akt or Erk, respectively [5,31]. Although Tie2 is a context-dependent regulator of blood vessel formation, how Akt or Erk activation is altered by Tie2 has not been determined so far.

Plasma membrane lipid raft domains, which contain high concentrations of cholesterol and sphingolipids, are known to function as centers for the assembly of signaling complexes. Such assembly is suggested to facilitate both specificity and the rate of signaling events, and it has become a central facet of signaling research as the function of many receptors and their downstream effectors are dependent on rafts [8–11]. Our present data show that raft disruption inhibits Akt phosphorylation but not Erk phosphorylation. We found that a subset of Tie2 becomes insoluble upon Ang1-stimulation. These results indicate that Tie2 localization or interaction on/with lipid rafts is key for regulation of Akt phosphorylation via Tie2 activation. Regulatory mechanisms, i.e. the joint strength between Tie2 and lipid rafts, types of lipid rafts or types of associated proteins with lipid rafts, may promote Tie2 localization to the raft domain. However, at present, the precise molecular mechanism regulating Tie2 localization to rafts is not known. Although the in vivo relevance of these findings remains to be proven, our experiments suggest that lipid rafts serve as signaling platforms for Tie2, separately controlling the Akt and Erk pathways, and that lipid rafts are important for signal transduction of Akt via Tie2 phosphorylation.

Several lines of research demonstrated that lipid raft disruption reduced basal Akt phosphorylation levels in tumor cells and that treatment with cholesterol-depleting agents such as mβCD induced apoptosis [31–34]. Moreover, it has been reported that lipid rafts contain junction proteins, such as annexin and VE-cadherin, in vascular ECs and that those proteins are recruited when cell-to-cell contact is established [35]. Cell–cell contact is one situation when cell apoptosis is inhibited, and Tie2 located on the cell–cell boundary preferentially induces Akt phosphorylation rather than Erk phosphorylation upon stimulation with Ang1 [5,31]. Akt, as described above, is important mediator for cell survival for ECs [18]. Therefore, when cell–cell contact is

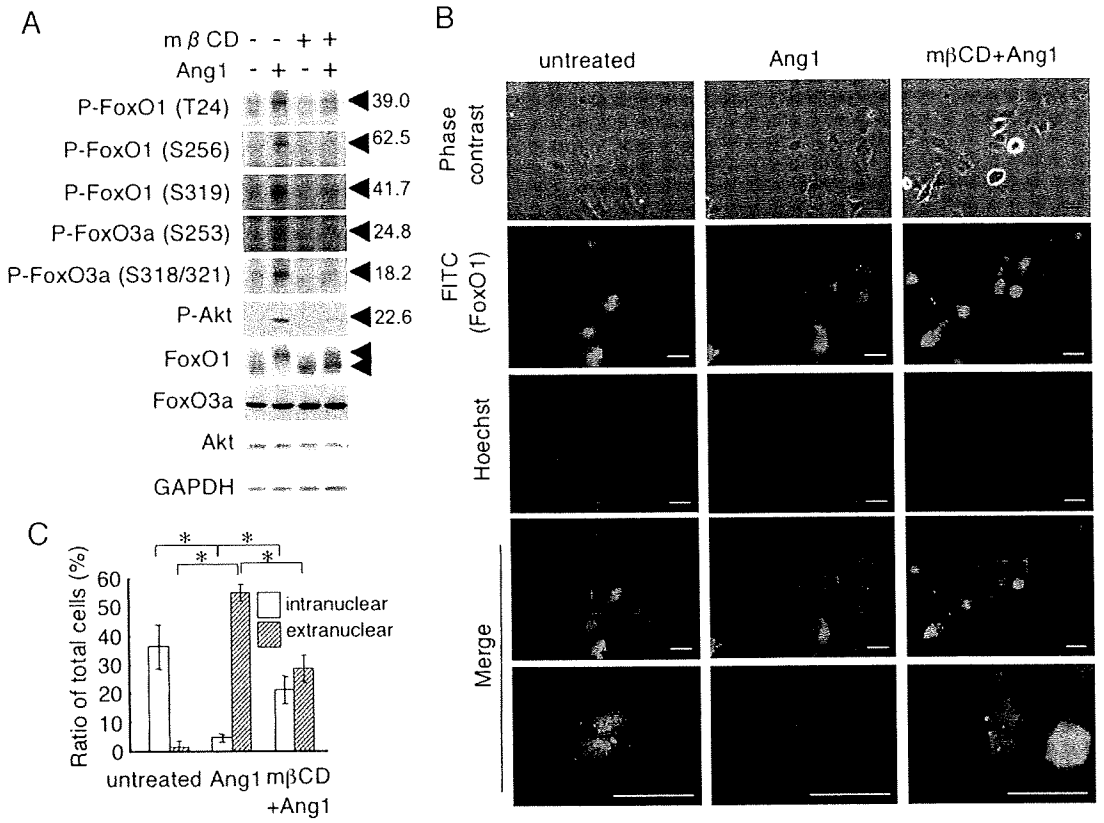

Fig. 4 – Lipid rafts serve as a signaling platform for the Tie2-FoxO pathway. (A) HUVECs were incubated with or without mβCD (10 mM) for 15 min and then stimulated with Ang1 (200 ng/mL) for 15 min. Total protein was subjected to immuno-blotting with the indicated antibodies. The density ratio is shown on the right side of each picture. To calculate the density ratio, the ratio of phosphorylated protein versus total protein was calculated for FoxO1, FoxO3a, and Akt protein. The ratio of Ang1-treated/mβCD-treated data to Ang1-treated/mβCD-untreated data is presented as a percentage for each. (B) HUVECs were incubated with or without mβCD (10 mM) for 15 min after serum starvation and then stimulated with Ang1 (200 ng/mL) for 30 min. Immunocytochemistry was performed after each treatment. Bottom panels show high power views indicated by a dashed box in each upper panel. Bar indicates 50 μm. (C) Quantitative evaluation of FoxO1 localization observed in (B). FoxO1 localization at the intranuclear or extranuclear part of the cell was scored and expressed as a percentage relative to total number of cells scored ($n=3$), *$P<0.01$.

established, recruitment of Akt to raft domain may be a key for regulation of EC survival via Tie2 activation.

At present, which molecules allow Tie2 to localize to lipid rafts are not known. One candidate is caveolin-1 because it is a major structural protein of caveolae, a subdomain of lipid rafts, and because the cytoplasmic domain of Tie2 contains a binding motif for caveolin-1 [36]. However, more precise analyses to identify the molecules that recruit Tie2 to lipid rafts will help to elucidate this mechanism.

In the present findings, we have provided evidence for the existence of a novel mechanism able to promote Akt signal transduction via Tie2 activation. Further precise molecular analyses of how Tie2 and Akt tether to lipid rafts may shed light on the mechanisms behind Tie2-dependent vascular quiescence and angiogenesis.

Acknowledgments

We thank K. Fukuhara for administrative assistance and N. Fujimoto for technical assistance. This work was partly supported by a Grant-in-Aid from The Ministry of Education, Culture, Sports, Science and Technology of Japan.

REFERENCES

[1] J. Folkman, Angiogenesis in cancer, vascular, rheumatoid and other disease, Nat. Med. 1 (1995) 27–31.
[2] D. Hanahan, J. Folkman, Patterns and emerging mechanisms of the angiogenic switch during tumorigenesis, Cell 86 (1996) 353–364.
[3] S. Davis, T.H. Aldrich, P.F. Jones, A. Acheson, D.L. Compton, V. Jain, T.E. Ryan, J. Bruno, C. Radziejewski, P.C. Maisonpierre, G.D. Yancopoulos, Isolation of angiopoietin-1, a ligand for the TIE2 receptor, by secretion-trap expression cloning, Cell 87 (1996) 1161–1169.
[4] C. Suri, P.F. Jones, S. Patan, S. Bartunkova, P.C. Maisonpierre, S. Davis, T.N. Sato, G.D. Yancopoulos, Requisite role of Angiopoietin-1, a ligand for the TIE2 receptor, during embryonic angiogenesis, Cell 87 (1996) 1171–1180.
[5] S. Fukuhara, K. Sako, T. Minami, K. Noda, H.Z. Kim, T. Kodama, M. Shibuya, N. Takakura, G.Y. Koh, N. Mochizuki, Differential function of Tie2 at cell–cell contacts and cell–substratum contacts regulated by angiopoietin-1, Nat. Cell Biol. 10 (2008) 513–526.

[6] K. Simons, E. Ikonen, Functional rafts in cell membranes, Nature 387 (1997) 569-572.
[7] D.A. Brown, E. London, Structure and function of sphingolipids- and cholesterol-rich membrane rafts, J. Biol. Chem. 275 (2000) 17221-17224.
[8] G. Werlen, E. Palmer, The TCR signalosome: a dynamic structure with expanding complexity, Curr. Opin. Immunol. 14 (2002) 299-305.
[9] B. Chini, M. Parenti, G-Protein coupled receptors in lipid rafts and caveolae: how, when and why do they go there? J. Mol. Endocrinol. 32 (2004) 325-338.
[10] R.S. Ostrom, P.A. Insel, The evolving role of lipid rafts and caveolae in G protein-coupled receptor signaling: implications for molecular pharmacology, Br. J. Pharmacol. 143 (2004) 235-245.
[11] J.A. Allen, R.A. Halverson-Tamboli, M.M. Rasenick, Lipid raft microdomains and neurotransmitter signalling, Nat. Rev. Neurosci. 8 (2007) 128-140.
[12] L.J. Pike, Lipid rafts: bringing order to chaos, J. Lipid Res. 44 (2003) 655-667.
[13] T. Okamoto, A. Schlegel, P.E. Scherer, M.P. Lisanti, Caveolins, a family of scaffolding proteins for organizing "preassembled signaling complexes" at the plasma membrane, J. Biol. Chem. 273 (1998) 5419-5422.
[14] L. Labrecque, I. Royal, D.S. Surprenant, C. Patterson, D. Gingras, R. Béliveau, Regulation of vascular endothelial growth factor receptor-2 activity by caveolin-1 and plasma membrane cholesterol, Mol. Biol. Cell 14 (2003) 334-347.
[15] D.A. Brown, J.K. Rose, Sorting of GPI-anchored proteins to glycolipid-enriched membrane subdomains during transport to the apical cell surface, Cell 68 (1992) 533-544.
[16] M.G. Tansey, R.H. Baloh, J. Milbrandt, E.M. Johnson Jr, GFRα-mediated localization of RET to lipid rafts is required for effective downstream signaling, differentiation, and neuronal survival, Neuron 25 (2000) 611-623.
[17] M.J. Yoon, C.H. Cho, C.S. Lee, I.H. Jang, S.H. Ryu, G.Y. Koh, Localization of Tie2 and phospholipase D in endothelial caveolae is involved in angiopoietin-1-induced MEK/ERK phosphorylation and migration in endothelial cells, Biochem. Biophys. Res. Commun. 308 (2003) 101-105.
[18] I. Kim, H.G. Kim, J.N. So, J.H. Kim, H.J. Kwak, G.Y. Koh, Angiopoietin-1 regulates endothelial cell survival through the phosphatidylinositol 3'-kinase/Akt signal transduction pathway, Circ. Res. 86 (2000) 24-29.
[19] B.P. Eliceiri, R. Klemke, S. Strömblad, D.A. Cheresh, Integrin αvβ3 requirement for sustained mitogen-activated protein kinase activity during angiogenesis, J. Cell. Biol. 140 (1998) 1255-1263.
[20] K.N. Meadows, P. Bryant, K. Pumiglia, Vascular endothelial growth factor induction of the angiogenic phenotype requires Ras activation, J. Biol. Chem. 276 (2001) 49289-49298.
[21] M. Potente, C. Urbich, K. Sasaki, W.K. Hofmann, C. Heeschen, A. Aicher, R. Kollipara, R.A. DePinho, A.M. Zeiher, S. Dimmeler, Involvement of Foxo transcription factors in angiogenesis and postnatal neovascularization, J. Clin. Invest. 115 (2005) 2382-2392.
[22] C. Daly, V. Wong, E. Burova, Y. Wei, S. Zabski, J. Griffiths, K.M. Lai, H.C. Lin, E. Ioffe, G.D. Yancopoulos, J.S. Rudge, Angiopoietin-1 modulates endothelial cell function and gene expression via the transcription factor FKHR (FOXO1), Genes Dev. 18 (2004) 1060-1071.
[23] A. Brunet, A. Bonni, M.J. Zigmond, M.Z. Lin, P. Juo, L.S. Hu, M.J. Anderson, K.C. Arden, J. Blenis, M.E. Greenberg, Akt promotes cell survival by phosphorylating and inhibiting a forkhead transcription factor, Cell 96 (1999) 857-868.
[24] G.J. Kops, N.D. De Ruiter, A.M. De Vries-Smits, D.R. Powell, J.L. Bos, B.M. Burgering, Direct control of the Forkhead transcription factor AFX by protein kinase B, Nature 398 (1999) 630-634.
[25] A. van der Horst, B.M. Burgering, Stressing the role of FoxO proteins in lifespan and disease, Nat. Rev. Mol. Cell Biol. 8 (2007) 440-450.
[26] Z. Tothova, D.G. Gilliland, FoxO transcription factors and stem cell homeostasis: insights from the hematopoietic system, Cell Stem Cell 1 (2007) 140-152.
[27] P.R. Somanath, O.V. Razorenova, J. Chen, T.V. Byzona, Akt1 in endothelial cell and angiogenesis, Cell Cycle 5 (2006) 512-518.
[28] M.J. Cross, L. Claesson-Welsh, FGF and VEGF function in angiogenesis: signalling pathways, biological responses and therapeutic inhibition, Trends Pharmacol. Sci. 22 (2001) 201-207.
[29] I. Shiojima, K. Sato, Y. Izumiya, S. Schiekofer, M. Ito, R. Liao, W.S. Colucci, K. Walsh, Disruption of coordinated cardiac hypertrophy and angiogenesis contributes to the transition to heart failure, J. Clin. Invest. 115 (2005) 2108-2118.
[30] T. Nagoshi, T. Matsui, T. Aoyama, A. Leri, P. Anversa, L. Li, W. Ogawa, F. del Monte, J.K. Gwathmey, L. Grazette, B. Hemmings, D.A. Kass, H.C. Champion, A. Rosenzweig, PI3K rescues the detrimental effects of chronic Akt activation in the heart during ischemia/reperfusion injury, J. Clin. Invest. 115 (2005) 2128-2138.
[31] P. Saharinen, L. Eklund, J. Miettinen, R. Wirkkala, A. Anisimov, M. Winderlich, A. Nottebaum, D. Vestweber, U. Deutsch, G.Y. Koh, B.R. Olsen, K. Alitalo, Angiopoietins assemble distinct Tie2 signalling complexes in endothelial cell-cell and cell-matrix contacts, Nat. Cell Biol. 10 (2008) 527-537.
[32] L. Zhuang, J. Lin, M.L. Lu, K.R. Solomon, M.R. Freeman, Cholesterol-rich lipid rafts mediate Akt-regulated survival in prostate cancer cells, Cancer Res. 62 (2002) 2227-2231.
[33] L. Zhuang, J. Kim, R.M. Adam, K.R. Solomon, M.R. Freeman, Cholesterol targeting alters lipid raft composition and cell survival in prostate cancer cells and xenografts, J. Clin. Invest. 115 (2005) 959-968.
[34] Y.C. Li, M.J. Park, S.K. Ye, C.W. Kim, Y.N. Kim, Elevated levels of cholesterol-rich lipid rafts in cancer cells are correlated with apoptosis sensitivity induced by cholesterol-depleting agents, Am. J. Pathol. 168 (2006) 1107-1118.
[35] S. Heyraud, M. Jaquinod, C. Durmort, E. Dambroise, E. Concord, J.P. Schaal, P. Huber, D. Gulino-Debrac, Contribution of annexin 2 to the architecture of mature endothelial adherens junctions, Mol. Cell. Biol. 28 (2008) 1657-1668.
[36] J. Couet, S. Li, T. Okamoto, T. Ikezu, M.P. Lisanti, Identification of peptide and protein ligands for the caveolin-scaffolding domain, J. Biol. Chem. 272 (1997) 6525-6533.

Tumor and Stem Cell Biology

Cancer Research

PSF1, a DNA Replication Factor Expressed Widely in Stem and Progenitor Cells, Drives Tumorigenic and Metastatic Properties

Yumi Nagahama[1], Masaya Ueno[1], Satoru Miyamoto[1], Eiichi Morii[2], Takashi Minami[4], Naoki Mochizuki[3], Hideyuki Saya[5], and Nobuyuki Takakura[1]

Abstract

PSF1 (partner of sld five 1) is an evolutionarily conserved DNA replication factor implicated in DNA replication in lower species that is strongly expressed in a wide range of normal stem cell populations and progenitor cell populations. Because stem and progenitor cells possess high proliferative capacity, we hypothesized that PSF1 may play an important role in tumor growth. To begin to investigate PSF1 function in cancer cells, we cloned the mouse PSF1 promoter and generated lung and colon carcinoma cells that stably express a PSF1 promoter-reporter gene. Reporter expression in cells correlated with endogenous PSF1 mRNA expression. In a tumor cell xenograft model, high levels of reporter expression correlated with high proliferative activity, serial transplantation potential, and metastatic capability. Notably, cancer cells expressing reporter levels localized to perivascular regions in tumors and displayed expression signatures related to embryonic stem cells. RNAi-mediated silencing of endogenous PSF1 inhibited cancer cell growth by disrupting DNA synthesis and chromosomal segregation. These findings implicate PSF1 in tumorigenesis and offer initial evidence of its potential as a theranostic target. *Cancer Res; 70(3); 1215–24. ©2010 AACR.*

Introduction

PSF1 (partner of SLD5) is a member of the tetrameric complex termed GINS, composed of SLD5, PSF1, PSF2, and PSF3, and is well conserved evolutionarily. In yeast, the GINS complex associates with the MCM2-7 complex and CDC45, and this "C-M-G complex" (CDC45-MCM2-7-GINS) regulates both the initiation and the progression of DNA replication (1–6). In *Xenopus* and human, GINS has been suggested to be involved in DNA replication because of its binding to DNA replication protein (7–10); however, a recent study suggests that PSF1/2 is associated with the response to replication stress and acquisition of DNA damage in untransformed human dermal fibroblasts (11). Thus, the exact functions of GINS components in mammalian cells are not yet clear.

Authors' Affiliations: [1]Department of Signal Transduction, Research Institute for Microbial Diseases, Osaka University; [2]Department of Pathology, Osaka University School of Medicine; [3]Department of Structural Analysis, National Cardiovascular Center Research Institute, Suita, Osaka, Japan; [4]Laboratory for Systems Biology and Medicine, Research Center for Advanced Science and Technology (LSBM), University of Tokyo, Meguro, Tokyo, Japan; and [5]Division of Gene Regulation, Institute for Advanced Medical Research, Keio University School of Medicine, Shinjyuku-ku, Tokyo, Japan

Note: Supplementary data for this article are available at Cancer Research Online (http://cancerres.aacrjournals.org/).

Corresponding Author: Nobuyuki Takakura, Department of Signal Transduction, Research Institute for Microbial Diseases, Osaka University, 3-1 Yamada-oka, Suita, Osaka 565-0871, Japan. Phone: 81-6-6879-8312; Fax: 81-6-6879-8314; E-mail: ntakaku@biken.osaka-u.ac.jp.

doi: 10.1158/0008-5472.CAN-09-3662

We have previously cloned the mouse ortholog of *PSF1* from a hematopoietic stem cell cDNA library (12) and found that PSF1 expression in mice was predominantly observed in the adult bone marrow and thymus, as well as the testis and ovary (i.e., tissues in which stem cell proliferation is actively induced and continues after birth). Moreover, we reported that PSF1 is strongly expressed in different immature cell lineages, such as cells in the inner cell mass during early embryogenesis as well as spermatogonia and hematopoietic stem cells after birth (12–14). Loss of PSF1 led to embryonic lethality around the implantation stage caused by the inability of cells of the inner cell mass to proliferate (12). Moreover, haploinsufficiency of PSF1 in $PSF1^{+/-}$ mice resulted in the delayed induction of hematopoietic stem cell proliferation during reconstitution of bone marrow after 5-fluorouracil ablation. These data strongly suggest that PSF1 is required for acute proliferation of cells, especially immature cells such as stem cells and progenitor cells.

Several recent studies have suggested that GINS components play a role not only in immature cells from normal tissues, as we reported, but also in cancer cells. For example, all GINS components were found to be overexpressed in intrahepatic cholangiocarcinoma tissues (15). A Gene Expression Omnibus (GEO) database search revealed that *PSF1* is an estrogen target in MCF7 human breast carcinoma cells (16). In a comprehensive study, it was found that *PSF1* and *SLD5* were upregulated in aggressive melanoma (17). Based on these results, we examined the nature of cells highly expressing PSF1 in a tumor xenograft model.

Genetic events caused by epigenetic modulation and microenvironmental exposure have been suggested to be responsible

for tumor progression. Therefore, a species-matched (murine) microenvironment is needed to examine the nature of cells strongly expressing PSF1.

Here, we have investigated the expression of PSF1 and the localization of PSF1-positive cancer cells in a mouse tumor cell xenograft model. We observed malignant behavior of highly PSF1-positive tumor cells with regard to tumorigenesis and metastasis. Moreover, highly PSF1-positive cancer cells have been characterized by microarray analysis, and the data compared with those of the recently reported embryonic stem cell (ESC)–like gene expression signature in poorly differentiated aggressive human tumors (18). Finally, to determine whether PSF1 could be a molecular target for the development of anticancer drugs, we silenced the *PSF1* gene by the RNA interference (RNAi) method in human carcinoma cell lines and observed the effects thereof on the growth of the cancer cells.

Materials and Methods

Cell culture and cell line construction. LLC, B16, NIH3T3, HeLa, and HEK293T were maintained in DMEM (Sigma) with 10% fetal bovine serum (FBS; Sigma) and penicillin/streptomycin (Life Technologies, Inc.). Colon26 cells were maintained in RPMI 1640 (Sigma) with 10% FBS and penicillin/streptomycin. Mouse embryonic fibroblasts were prepared from day 14.5 embryos and cultured in high-glucose DMEM (Sigma) with 10% FBS and penicillin/streptomycin.

The gene encoding the PSF1 promoter region was isolated by mouse BAC cloning (RP23-193L22, Advanced GenoTechs Co.). Using the 5′ upstream sequence of the first exon of the *PSF1* locus as a probe, 5.5 kb of the 5′flanking PSF1 gene were isolated and subcloned into pBluescript II KS (Stratagene). The enhanced green fluorescent protein (*EGFP*) gene and the *neomycin* gene were excised from pEGFP-N1 and pcDNA3.1(−) (Clontech), respectively, and ligated to the 5.5 kb of the PSF1 5′-flanking fragment. This construct was designated *PSF1p-EGFP*. LLC and colon26 cells were transfected using Lipofectamine 2000 (Invitrogen). After transfection, the cells were cultured in medium supplemented with G418 (Life Technologies) to obtain cells stably expressing EGFP under the control of the PSF1 promoter (LLC-*PSF1p-EGFP* and colon26-*PSF1p-EGFP*).

Quantitative reverse transcription-PCR. Quantitative reverse transcription-PCR (RT-PCR) was done as previously described (14). The primer sets were described in Supplementary Materials and Methods.

Mice. Seven- to eight-week-old C57BL/6 female mice (for the LLC experiments) and BALB/c female mice of the same age (for colon26) were purchased from Japan SLC. All animal studies were approved by the Osaka University Animal Care and Use Committee. Subcutaneous xenografts were established by injecting 10^6 cells into the flanks of the mice.

Flow cytometric analysis. Single-cell suspensions from tumors were prepared using a standard protocol. Cell sorting was done using a FACSAria (Becton Dickinson). For the EGFP^{high} population, the 5% most brightly fluorescing cells were sorted, and for the EGFP^{low} population, the 5% least fluorescent. We used parental LLC or colon26 as negative controls.

In vitro *clonal analyses and* in vivo *tumorigenicity analysis.* Isolated cells were plated on 10-cm culture dishes (200 per dish for LLC-*PSF1p-EGFP* and 100 per dish for colon26-*PSF1p-EGFP*) and cultured. The percentage of cells that initiated a clone was taken as the plating efficiency. For *in vivo* experiments, 100 sorted cells in 100 μL of PBS with growth factor–reduced Matrigel (BD Biosciences; 1:1) were injected s.c. into the mice. Five weeks after injection, tumor volumes were measured with a caliper and calculated as width × width × length × 0.52.

Invasion assay and metastasis assay. The invasive activity of tumor cells was assayed using a BioCoat Matrigel Invasion Chamber (BD Biosciences) according to the manufacturer's instruction.

For the lung metastasis assay using LLC-*PSF1p-EGFP*, 10^5 viable sorted cells were injected into the tail veins of mice. After 4 wk, lungs were dissected and the number of colonies observable on the surface of the lungs was noted. For the hepatic metastasis assay of colon26-*PSF1p-EGFP*, spleens of mice were exposed to allow the direct injection of 5×10^4 viable sorted cells. After 12 d, livers and spleens were dissected out and the number of colonies observable on the surface of the livers was recorded. Sections of liver were stained with H&E to evaluate tissue morphology and to detect metastases.

Immunohistochemistry and immunocytochemistry. Immunohistochemical analyses were done as previously described (19). Rabbit anti-GFP antibody (Invitrogen) and rat anti-CD31 (BD Biosciences) were used for primary antibodies. For the fluorescent immunohistochemical analyses, phycoerythrin-conjugated anti-CD31 (BD Biosciences) was used for staining endothelial cells.

For immunocytochemistry, anti-PSF1(14), anti-bromodeoxyuridine (BrdUrd) (Zymed Laboratories), anti–β-tubulin (Sigma), anti–CENP-A (MBL), and anti-survivin (Chemicon International, Inc.) antibodies were used as previously described (14).

PSF1 *knockdown.* Transfection was done using Lipofectamine 2000 (Invitrogen). For the enrichment of transiently shRNA vector–transfected cells, the puromycin resistance gene was ligated into the *Xho*I site of the pSINsi-hU6 vector (Takara), and then sense and antisense oligonucleotide pairs (see below) were annealed and ligated into the *Bam*HI/*Cla*I site of the pSINsi-hU6-P vectors. The sequences of the oligonucleotide sets were described in Supplementary Materials and Methods. For time-lapse imaging of histone H3 and tubulin in living cells, HEK293T cells were transfected with GFP-histone (20) or tubulin-GFP (Clontech) expression vectors, and stably expressing clones were selected. Time-lapse observation was done as previously reported using an IX70 microscope (Olympus; ref. 21).

Microarray and bioinformatics analysis. Microarrays were done as previously described (22). Raw data are available for download from GEO (GSE17112). Gene set enrichment analysis (GSEA; ref. 23) was done by CeresBioscience as previously reported.

Statistical analysis. Results were expressed as the mean ± SEM. Student's *t* test was used for statistical analysis. Differences were considered statistically significant when $P < 0.01$.

Results

Establishment of transgenic cell lines to monitor endogenous* PSF1 *expression in living cells. We first examined *PSF1* mRNA expression in mouse cancer cell lines, a noncancer cell line, and primary cultured cells. *PSF1* mRNA in cancer cell lines is expressed to a greater degree than in the noncancer cell line or primary cultured cells (Fig. 1A). To determine whether the cancer cells strongly expressing PSF1 had malignant features, they need to be collected as living cells. Because PSF1 is an intracellular protein, viable cells cannot be isolated using PSF1 antibody and flow cytometric cell sorting. Therefore, we used promoter activity to monitor the expression level of PSF1 in cancer cells in the murine tumor xenograft model. We have cloned the mouse *PSF1* promoter gene and established lung carcinoma [Lewis lung carcinoma (LLC)] and colon cancer (colon26) cell lines stably expressing EGFP under the transcriptional control of the *PSF1* promoter (LLC- and colon26-*PSF1p-EGFP*, respectively). We confirmed *PSF1* mRNA expression in parental LLC and colon26 cells (data not shown). After inoculation of LLC-*PSF1p*-EGFP, tumors were dissected and the intensity of EGFP in dissociated cancer cells was analyzed by flow cytometry (Fig. 1B–D). As can be seen, EGFP-positive ($EGFP^+$) cells containing high or low levels of EGFP ($EGFP^{high}$ or $EGFP^{low}$ cells, respectively) were present. These were separated and the expression of *PSF1* mRNA was examined (Fig. 1D). The results indicate that the intensity of EGFP is correlated with the endogenous *PSF1* expression. Similar results were obtained using colon26-*PSF1p-EGFP* (data not shown). These results suggest that these cell lines are useful tools to monitor endogenous *PSF1* expression in living cells.

EGFP(PSF1)^{high} cells possess greater tumorigenic capacity. To study their colony forming efficiency, cancer cells

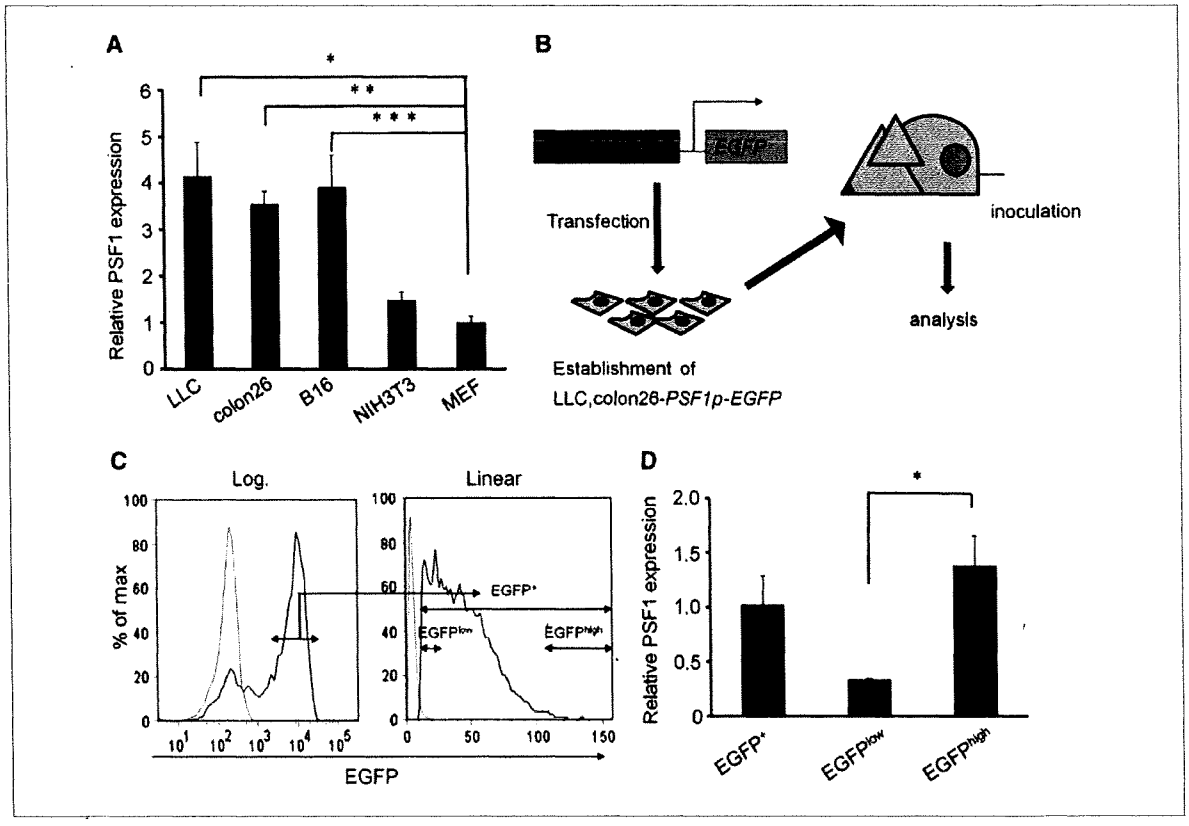

Figure 1. PSF1 expression in murine carcinoma cell lines. A, expression of *PSF1* mRNA in murine carcinoma cells. Total RNA was analyzed by quantitative RT-PCR for *PSF1* expression in different murine carcinoma cell lines and compared with a noncancer cell line and a primary cell culture. The values are normalized to the amount of mRNA in mouse embryonic fibroblasts. *LLC*, lung carcinoma; *colon26*, colon carcinoma; *B16*, melanoma; *NIH3T3*, mouse embryonic fibroblast cell line; *MEF*, mouse embryonic fibroblast. Data show the mean ± SEM. *, **, ***, $P < 0.01$ ($n = 3$). B, experimental procedure. We have cloned the mouse *PSF1* promoter gene and established cell lines stably expressing EGFP under the transcriptional control of the *PSF1* promoter (LLC- and colon26-*PSF1p-EGFP*, respectively). After inoculation of LLC- or colon26-*PSF1p*-EGFP, tumors were dissected and the dissociated cancer cells were separated using a cell sorter according to the intensity of EGFP expression and further analyzed. C, fluorescence-activated cell sorting analysis of cells from tumor tissues injected with LLC (green) or LLC-*PSF1p-EGFP* (red) cells. $EGFP^+$, $EGFP^{low}$, and $EGFP^{high}$ cells were sorted as indicated. Intensity of EGFP is displayed on a log or linear scale. D, quantitative RT-PCR analysis of *PSF1* mRNA expression in sorted cells as indicated. The values are normalized to the amount of mRNA in $EGFP^+$ cells. Data show the mean ± SEM. *, $P < 0.01$ ($n = 3$).

(LLC- and colon26-*PSF1p-EGFP*) from tumor-bearing mice were divided into three fractions (EGFP$^+$, EGFP^{low}, and EGFP^{high}) as indicated in Fig. 1C, seeded, and cultured for 2 weeks. EGFP^{high} cells formed significantly larger colonies than did EGFP^{low} cells (Fig. 2A) in both colon26 and LLC tumors.

We next examined the serial transplantation ability of these cells. We inoculated sorted EGFP^{high} or EGFP^{low} cells from tumor-bearing mice into new hosts to evaluate the relationship between PSF1 expression and tumorigenicity. Four weeks (LLC-*PSF1p-EGFP*) or 2 weeks (colon26-*PSF1p-EGFP*) after initial inoculation, 100 sorted EGFP$^+$, EGFP^{low}, or EGFP^{high} tumor cells were again transplanted into new hosts. EGFP^{high} cells from both LLC and colon26 tumors formed significantly larger tumors than did EGFP^{low} or EGFP$^+$ cells (Fig. 2B). When tumor cell components were examined in tumors generated after the second transplantation, EGFP^{high} cells were found to have given rise to both EGFP^{high} and EGFP^{low} cells in both LLC and colon26 tumors (Supplementary Fig. S1). Taken together, these data suggest that cancer cells expressing higher levels of *PSF1* exhibit high cloning efficiency and tumorigenicity.

EGFP(PSF1)^{high} cells possess greater invasive and metastatic capacity. We investigated that EGFP^{high} cells also play a crucial role in tumor metastasis. We determined the overall ability of cells sorted, as described in Fig. 1C, for invasion using Matrigel, a basement membrane model used to estimate metastatic potential. EGFP^{high} cells migrated more effectively than did EGFP^{low} cells or EGFP$^+$ cells, indicating that they possess greater invasive capacity (Fig. 3A and B).

Next, we examined the *in vivo* metastatic potential of these cells by two different means. First, viable sorted EGFP^{high} or EGFP^{low} cells from LLC tumors were injected into the tail veins of recipient mice. After 4 weeks, macrometastatic lesions

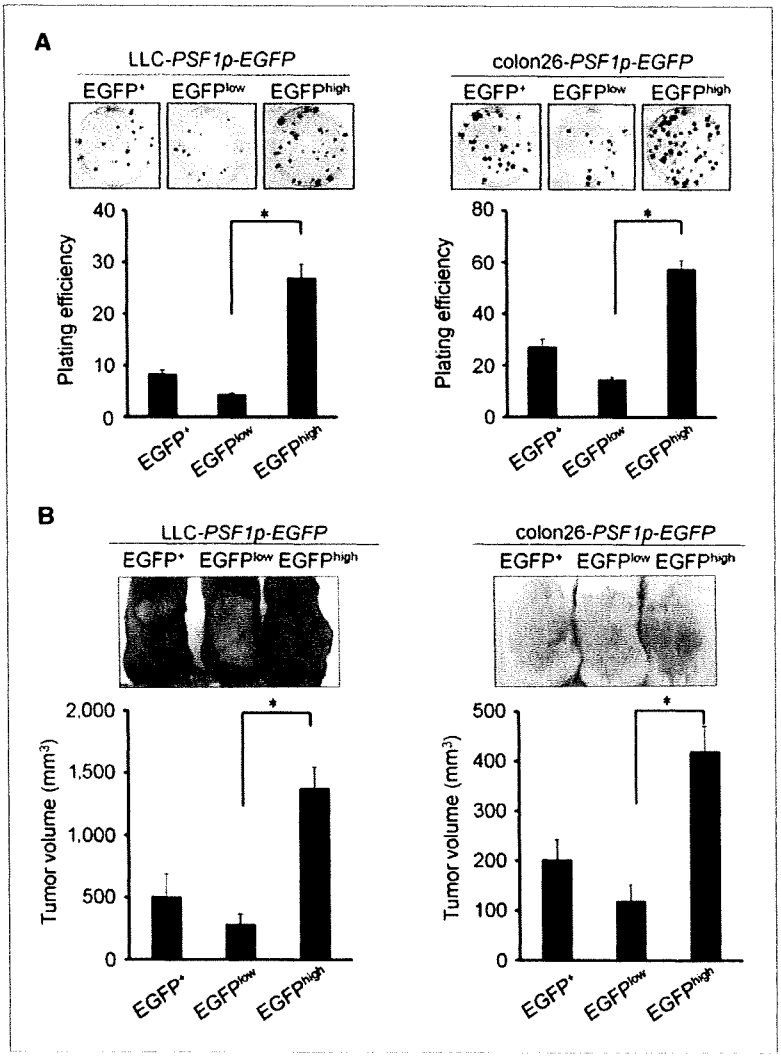

Figure 2. High proliferative ability of PSF1^{high} cancer cells. A, plating efficiency of sorted cells. Sorted cells from tumor tissues injected with LLC-*PSF1p-EGFP* or colon26-*PSF1p-EGFP* were seeded onto 10-cm culture dishes and cultured for 2 wks. Colonies generated from different fractions as indicated were stained with Giemsa solution (top). Quantitative evaluation of colonies from each fraction as indicated. Percentages of the colony numbers relative to the number of cells seeded are presented (bottom). Data show the mean ± SEM. *, $P < 0.01$ ($n = 3$). Results shown are representative of at least three independent experiments. B, tumorigenesis assay. Gross appearance of the tumor mass in mice 5 wks after inoculation with sorted cancer cells as indicated (top). Tumor volume was determined 5 wks after inoculation with sorted cells as indicated (bottom). Data show the mean ± SEM. *, $P < 0.01$ ($n = 10$). Experiments were done at least three times with similar results.

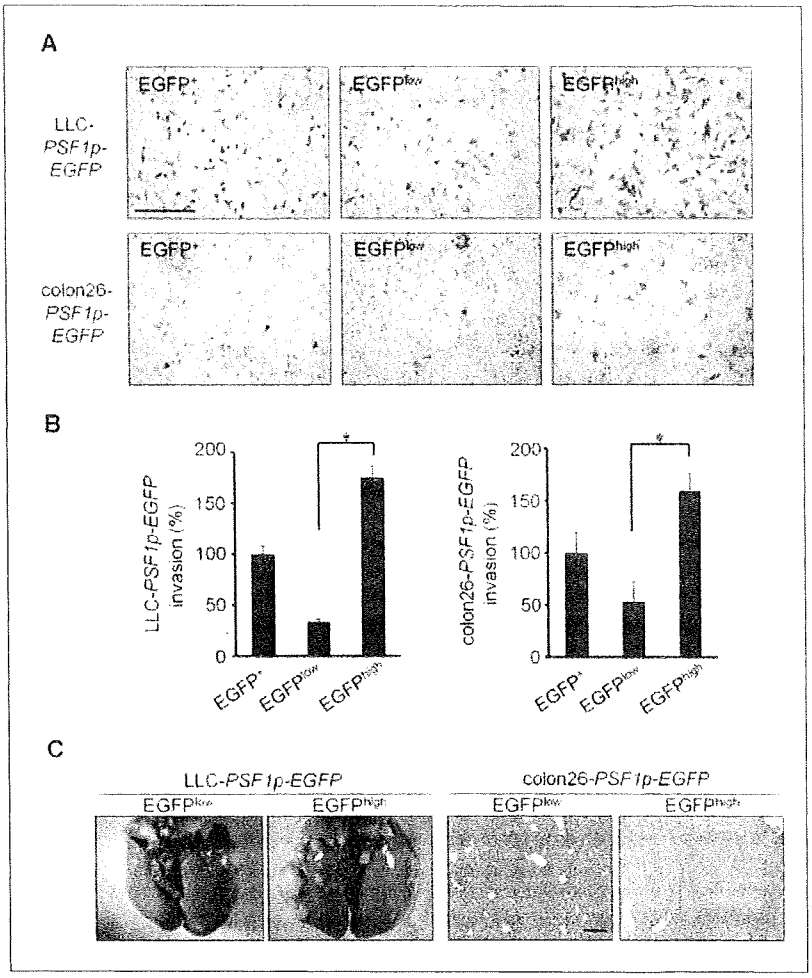

Figure 3. Invasive and metastatic capacity of LLC-*PSF1p-EGFP* and colon26-*PSF1p-EGFP*. A, representative images of sorted cells that migrated across a Matrigel-coated membrane. Bar, 200 μm. B, quantitative evaluation of the migrated cells: percentage of migrated cells relative to the applied total cell number normalized with the data from EGFP$^+$ cells. Data show the mean ± SEM. *, $P < 0.01$ ($n = 3$). Results shown are representative of at least three independent experiments. C, metastasis analysis. Gross appearance of lung metastases after injection with sorted EGFP^{low} or EGFP^{high} cells from LLC tumor (left). Liver metastases after injection with sorted EGFP^{low} or EGFP^{high} cells from colon26 tumor (right). Bar, 200 μm. Results shown are representative of at least three independent experiments.

in the lung were enumerated. Results clearly indicated that EGFP^{high} cells had a higher metastatic potential than did EGFP^{low} cells (Fig. 3C; Supplementary Fig. S2A). Second, in the case of colon26 tumors, viable sorted EGFP^{high} or EGFP^{low} cells were injected into the spleen. After 12 days, metastatic nodules in the liver were analyzed on liver sections. EGFP^{low} cells rarely generated metastatic foci, but large lesions were frequently observed in the livers of mice injected with EGFP^{high} cells (Fig. 3C; Supplementary Fig. S2B).

ESC-like signatures are enriched in EGFP^{high} cells versus EGFPlow cells. Recent studies showed that poor prognosis in a diverse set of human and mouse malignancies is associated with the expression of an ESC-like genetic program (18). We therefore compared the gene expression signatures of EGFP^{low} and EGFP^{high} cells. Data clearly indicated that ESC-like signatures were enriched in EGFP^{high} cells versus EGFP^{low} cells (Fig. 4). Interestingly, other ESC-like signatures (24, 25), in which some cancer-initiating/stem cells (CIC/CSC) were enriched, were also enriched in EGFP^{high} cells versus EGFP^{low} cells (Fig. 4; Supplementary Table S1). Taken together, the results from all the above experiments lead us to conclude that cancer cells harboring large amounts of PSF1 or high transcriptional activity of *PSF1* possess malignant features, including high proliferative capacity, tumorigenesis, metastatic ability, and genetic profiles of poor prognosis.

PSF1^{high} cells are localized in perivascular regions. Next, the tissue distribution of EGFP^{high} cells in tumors was examined (Fig. 5A–C). EGFP^{high} cells were located close to the edge of the tumor and near the blood vessels. Preliminary, we investigated PSF1 expression in human carcinoma specimens (Supplementary Fig. S3). We found that PSF1 expression in human lung and esophageal squamous cell carcinoma specimens was confined to the surrounding basal-like cells and located at some distance from the centers of terminal differentiation zones. Furthermore, PSF1-positive cells were located in close proximity to blood vessels near the edge of the tumor, as observed in our murine xenograft model (Supplementary Fig. S3).

Silencing of PSF1 inhibits the proliferation of carcinoma cells. Targeted disruption of PSF1 led to embryonic lethality

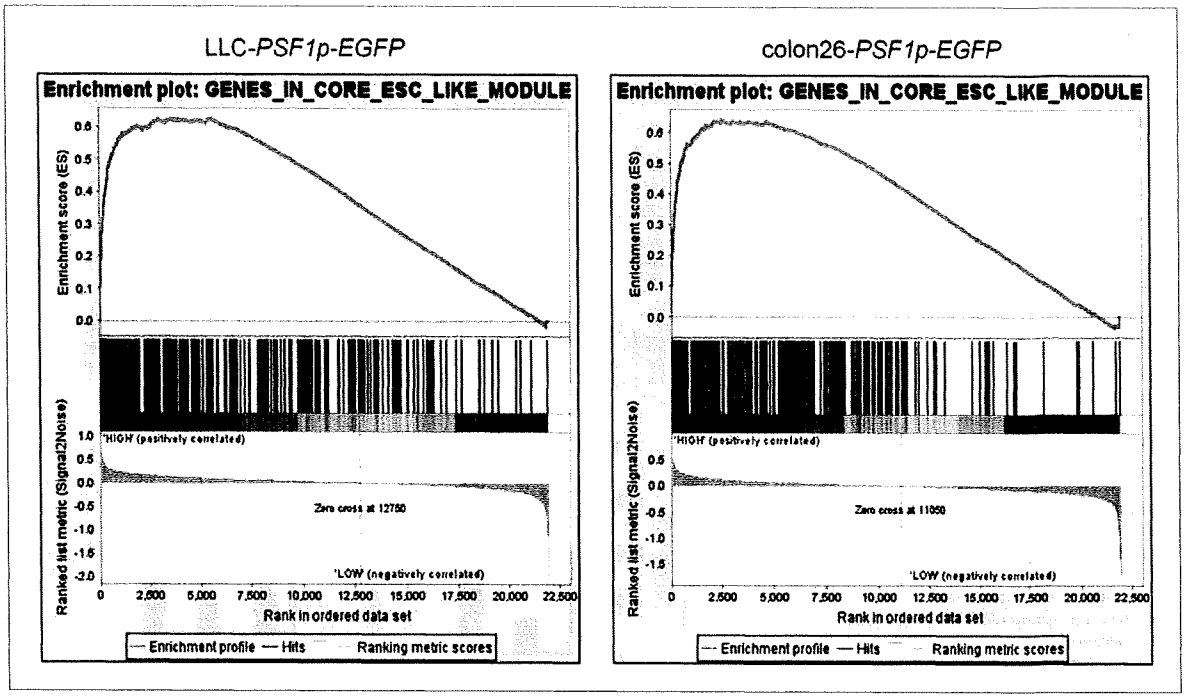

Figure 4. Gene set enrichment analysis. GSEA plots show that expression of an ESC-like core gene module (24) is more enriched in EGFP^{high} cells compared with EGFP^{low} cells in LLC-*PSF1p-EGFP* tumor and colon26-*PSF1p-EGFP* tumor.

caused by the inhibition of cell growth in the inner cell mass (12), suggesting that silencing this gene may also inhibit tumor cell proliferation. To determine whether PSF1 could be a suitable molecular target for anticancer drug development, the inhibitory effects of its expression in human carcinoma cell lines should be evaluated. In budding yeast, it has been suggested that PSF1 plays a role in DNA replication, associated with the formation of the DNA replication fork (7–9). However, its function in mammalian cells has not been clarified. First, we established the cellular localization of PSF1 in HeLa cells (Fig. 6A). At interphase, PSF1 was localized predominantly in the nuclei. During mitosis, it was almost exclusively diffusely located outside the chromatin. Next, we used short hairpin RNA (shRNA) expression plasmids for RNAi-mediated endogenous gene silencing in HeLa cells *in vitro*. Quantitative RT-PCR with gene-specific shRNA confirmed that endogenous PSF1 gene expression was reduced by more than 75% within 72 hours, compared with the lack of effect of transfection of a scrambled shRNA expression plasmid (data not shown). At 96 hours, the total number of PSF1 shRNA–treated cells was significantly decreased compared with the control (Fig. 6B), suggesting that depletion of PSF1 had resulted in cell growth arrest. To analyze more precisely the effect of PSF1 depletion on cell growth, first, the DNA contents were analyzed (Fig. 6C, left). Results showed that depletion of PSF1 led to an increase in the fraction of cells in the sub-G_1, S, and G_2-M phases, suggesting that this molecule is important not only for S phase but also for G_2-M phase progression.

Polyploid cells can arise as a result of errors in mitosis. These cells usually exit the cycle in an aberrant fashion, without sister chromatid segregation or cytokinesis, a process known as "mitotic slippage." Cancer cell lines (such as HeLa and HEK293T cells) lacking functional p53 progress into S phase without p53-dependent growth arrest at the subsequent G_1-S boundary, and hyperploid cells develop as a result. However, no obvious hyperploid cell populations were found in PSF1-depleted cells (Fig. 6C, left). During a 4-hour pulse, approximately 75% of scrambled shRNA–treated cells incorporated BrdUrd (Fig. 6C, right), but only approximately 23% of PSF1-depleted cells possessed large nuclei staining with anti-BrdUrd antibody. Taken together, these data indicate that PSF1 depletion also inhibits DNA synthesis of multiploid cells, which resulted in the generation of only a small number of cells harboring large nuclei (8N; Fig. 6C, left).

During the 72- to 120-hour period after shRNA treatment, the population of G_2-M phase cells increased in the PSF1 depletion experiments (Fig. 6C, left). Therefore, we assessed the function of PSF1 in G_2-M progression. In the scrambled shRNA–treated control population, most cells had divided within 60 minutes, whereas division times were prolonged in the PSF1-depleted cells (Fig. 6D, left). To examine this in terms of chromosome segregation, real-time imaging was done with histone H2B-GFP, which labels the chromosomes (Fig. 6D, middle). In control cells, the chromosomes were condensed and congressed to the metaphase plate, but subsequently, and suddenly, they completely segregated and the

time spent in metaphase was between 15 and 30 minutes. By contrast, PSF1 depletion prolonged the duration of metaphase by between 33 and 145 minutes, and a proportion of the PSF1-depleted cells showed abnormal chromosome congression and segregation (data not shown). Real-time observation with GFP-tubulin also revealed that depletion of PSF1 caused arrest at metaphase (data not shown). To resolve whether this mitotic arrest, induced by PSF1 depletion, was dependent on the spindle assembly checkpoint, Mad2 was co-depleted from the cells. We found that the mitotic arrest of almost all co-depleted cells was rescued by the early onset of anaphase (Fig. 6D, right). Taken together, these data showed that, in the absence of PSF1, the spindle checkpoint signal was activated and mitotic arrest was precipitated.

Because we observed abnormalities in metaphase arrest and DNA segregation in PSF1-depleted cells, we next analyzed spindle organization by staining for β-tubulin. Results showed that approximately 10% of the mitotic cells formed multipolar asters (Fig. 6E, left), whereas a small number of abnormal spindles were found in the control experiments (data not shown). Moreover, by immunostaining with anti-survivin antibody, we found that unaligned chromosomes were present in PSF1 shRNA–treated cells, which may reflect a defect in chromosome congression or segregation (Fig. 6E, middle). Recently, we reported that PSF1-deficient mice were nonviable at around embryonic day E6.5 and that BrdUrd incorporation was inhibited in the cultured inner cell mass from the blastocysts of E3.5 *PSF1*$^{-/-}$ embryos (12). Consistent with the present results from RNAi experiments in HeLa cells, we found that micronuclei and abnormal chromosomal segregation occurred in E3.5 *PSF1*$^{-/-}$ blastocysts (Fig. 6E, right). These data indicate that PSF1 contributes not only

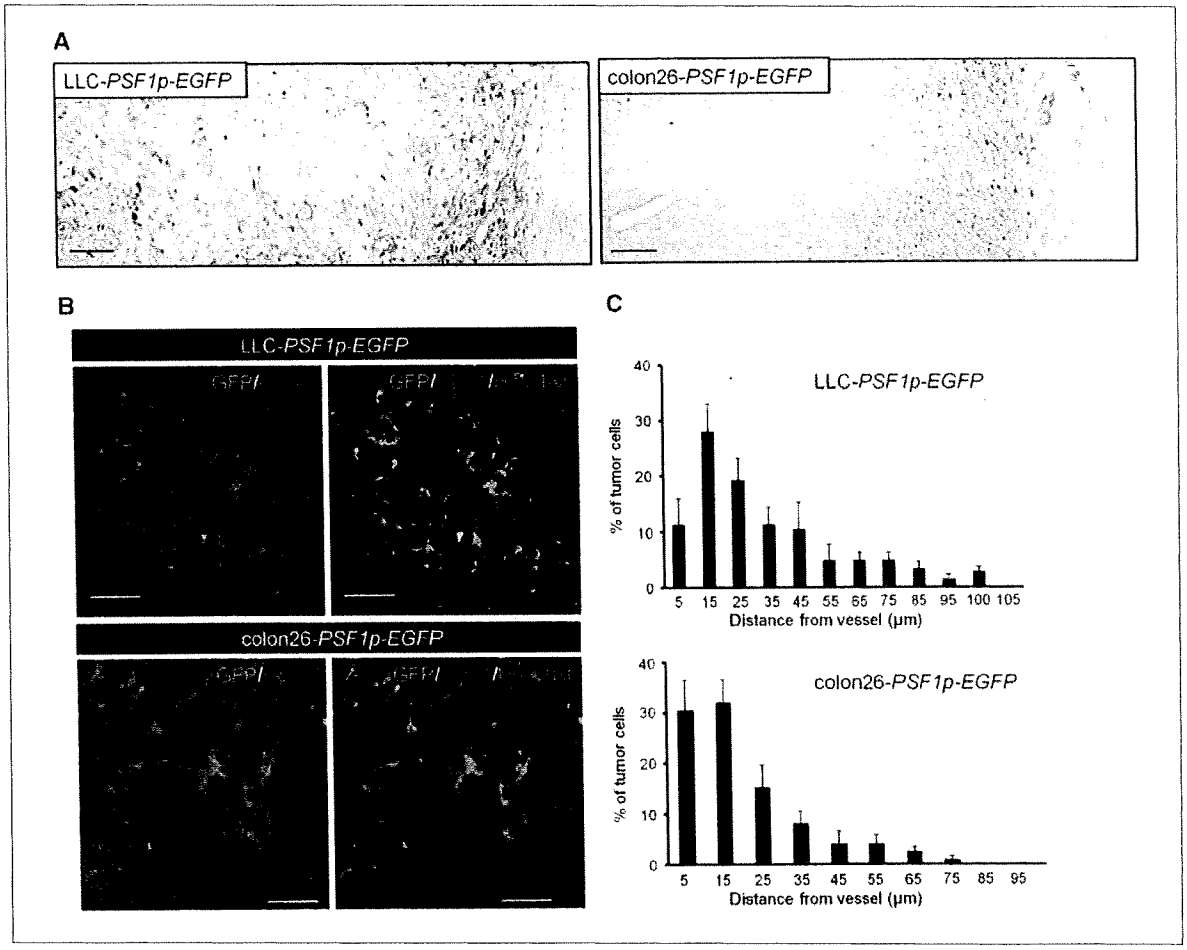

Figure 5. Localization of cancer cells strongly expressing PSF1. A, sections from LLC-*PSF1p-EGFP* (left) and colon26-*PSF1p-EGFP* (right) xenografts were double stained with anti-GFP antibody (brown in left, purple in right) and anti-CD31 antibody (red). Bar, 100 μm. B, sections of LLC-*PSF1p-EGFP* (top) and colon26-*PSF1p-EGFP* (bottom) tumor tissues were stained with anti-CD31 antibody (red). Nuclei were counterstained with Hoechst 33342 (blue). Endogenous EGFP was observed in low contrast (left) and high contrast (right). C, percentages of EGFP^{high} cells that were located at incremental distances of 5 μm from the nearest CD31^{+} endothelial cells. Data are mean ± SEM from five random fields. Bar, 100 μm.

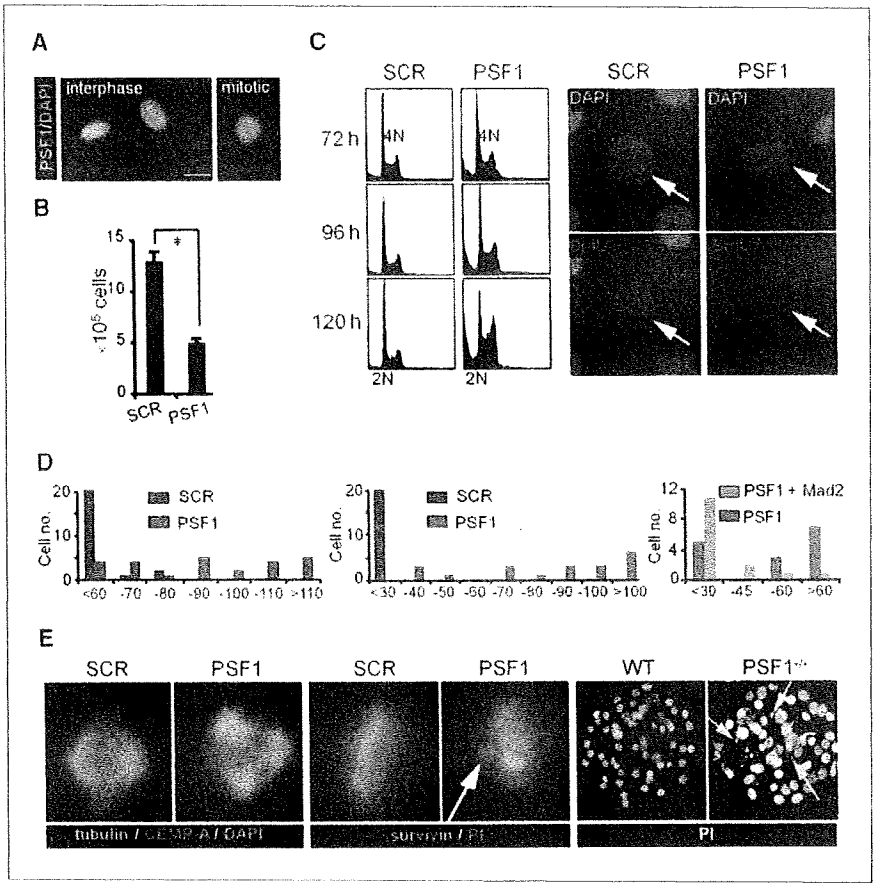

Figure 6. *PSF1* silencing inhibits proliferation of cancer cells. A, HeLa cells were immunostained with anti-PSF1 (green). DNA was counterstained with 4',6-diamidino-2-phenylindole (DAPI; blue). B, total numbers of RNAi-treated HeLa cells 96 h after transfection (bottom). *SCR*, nonspecific scrambled shRNA as a negative control. *, $P < 0.05$. C, DNA content of shRNA-treated HeLa cells (72 h after transfection) was determined by flow cytometry (left). DNA synthesis in large nucleated cells treated with the indicated shRNA. Immunostaining was done with anti-BrdUrd antibody (red), and counterstaining with DAPI (blue; right). Arrows, large nuclei. D, HeLa cells were treated with control (blue) or PSF1 (red) shRNA. Time required for cell division was evaluated by time-lapse observation 72 to 96 h after transfection (left). Using histone H3-GFP–expressing HEK293T cells, metaphase retention time was observed 72 to 120 h after transfection (middle). The H3-GFP-HEK293T cells were cotransfected with PSF1 shRNA and scrambled shRNA (red) or PSF1 and Mad2 shRNA vectors (green), and metaphase retention time was observed 36 to 72 h after transfection (right). E, HeLa cells transfected with shRNA as indicated. Expression of tubulin (green) and CENP-A (red; left). DNA was counterstained with DAPI (blue). Expression of survivin (green; middle). DNA was counterstained with propidium iodide (red). E3.5 $PSF1^{+/+}$ or $PSF1^{-/-}$ embryos were fixed and stained with propidium iodide (right). Arrows, disorganized micronuclei.

to DNA replication but also to the transition from metaphase to anaphase, as well as to chromosome segregation.

Discussion

In the present work, we used cells with a high level of expression of PSF1 to show that these malignant cancer cells, which are located in the vascular region and at the edge of the tumor, exhibit high tumorigenic and metastatic ability.

Thus far, acquisition of genetic changes affected by epigenetic manipulation and microenvironmental exposure has been suggested to be responsible for tumor progression. When we cultured the tumor cells *in vitro*, we observed that the population consisted of PSF1(EGFP)^{high} and PSF1(EGFP)^{low} fractions. When sorted and separately injected into mice, we failed to detect any marked differences between them in terms of tumorigenic or metastatic capacity (data not shown). When nonfractionated tumor cells from these cultures were injected, the tumors that developed consisted of both PSF1(EGFP)^{high} and PSF1(EGFP)^{low} cells. However, when these cells extracted from tumors *in vivo* were fractionated into PSF1(EGFP)^{high} and PSF1(EGFP)^{low} and injected into mice again, then we did see clear a difference in terms of tumorigenic and metastatic capacity between the two fractions.

Our model therefore strongly supports the possibility that environmental changes *in vivo* clearly affect the features of cancer cells with regard to tumorigenicity or nontumorigenicity. Thus, this model suggested that the interaction of cancer

cells with their microenvironment changes them into more malignant ones. In our tumor model as well as histology of human tissues, cells highly positive for PSF1 are located near blood vessels. It has been suggested that CSCs/CICs localize in the perivascular region (26), as is observed in normal organs, where stem cells are located in the vascular niche (27). Furthermore, microarray data clearly indicated that ESC-like signatures, which are reported to be enriched in CSCs/CICs fractions, were also enriched in $EGFP^{high}$ cells versus $EGFP^{low}$ cells (Fig. 4). Thus, the subpopulation of cells strongly positive for PSF1 might include the CSC/CIC fraction.

Antitumor angiogenesis is a promising approach for managing cancer patients, and many angiogenesis-disrupting agents have been developed (28). Although some agents have already been tested clinically and prolongation of survival has been confirmed, it is impossible to destroy all of the blood vessels in a tumor. Recent research in mice has suggested that the tumor repopulates from the edge region to the center after treatment with an angiogenesis-disrupting agent (28), and also that malignant tumor cells egress through remnant blood vessels at the tumor edge after inhibition of vascular endothelial growth factor signals (29). We previously reported that blood vessels in peripheral regions of tumors are well matured compared with those in the center and that they are resistant to antiangiogenic drugs (19, 30). Our data therefore strongly support the notion that cells with malignant features located near blood vessels at the tumor edge and showing resistance to angiogenesis-disrupting agents are responsible for invasion and metastasis. Our present model represents a precise analytic tool to determine whether candidate drugs directed against cells with malignant features including CSCs/CICs or blood vessels actually do suppress proliferation of cancer cells or destroy the vascular niche.

Our data clearly indicate that PSF1 plays a pivotal role in DNA replication and microtubule organization. Recently, it has been suggested that molecules homologous with those associated with DNA replication in lower species also regulate other cellular events in mammalian cells (31–33). In higher eukaryotes, a number of environmental cues affecting cell division involve DNA replication proteins that are also used by lower eukaryotes and that perform diverse functions in cytokinesis. Therefore, there is a possibility that, in addition to its role in microtubule organization, which we have shown here, plus the known part it plays in DNA replication, PSF1 may also have other cellular functions in symmetrical or asymmetrical cell division of malignant cancer cells by influencing cell structure. As we showed here, the possibility that PSF1 is expressed by malignant cancer cells, which may include CSCs or CICs, and the finding that silencing PSF1 induced cancer cell apoptosis suggest that this molecule may represent an important new target for the development of anticancer drugs.

Disclosure of Potential Conflicts of Interest

No potential conflicts of interest were disclosed.

Acknowledgments

We thank N. Fujimoto and K. Fukuhara for technical assistance, and A. Taguchi for technical assistance with the microarray analysis.

Grant Support

Japanese Ministry of Education, Culture, Sports, Science and Technology and the Japanese Society for Promotion of Science.

The costs of publication of this article were defrayed in part by the payment of page charges. This article must therefore be hereby marked *advertisement* in accordance with 18 U.S.C. Section 1734 solely to indicate this fact.

Received 10/7/09; revised 11/25/09; accepted 12/3/09; published OnlineFirst 1/26/10.

References

1. Takayama Y, Kamimura Y, Okawa M, Muramatsu S, Sugino A, Araki H. GINS, a novel multiprotein complex required for chromosomal DNA replication in budding yeast. Genes Dev 2003;17:1153–65.
2. Bauerschmidt C, Pollok S, Kremmer E, Nasheuer HP, Grosse F. Interactions of human Cdc45 with the Mcm2-7 complex, the GINS complex, and DNA polymerases δ and epsilon during S phase. Genes Cells 2007;12:745–58.
3. Gambus A, Jones RC, Sanchez-Diaz A, et al. GINS maintains association of Cdc45 with MCM in replisome progression complexes at eukaryotic DNA replication forks. Nat Cell Biol 2006;8:358–66.
4. Kanemaki M, Sanchez-Diaz A, Gambus A, Labib K. Functional proteomic identification of DNA replication proteins by induced proteolysis *in vivo*. Nature 2003;423:720–4.
5. Moyer SE, Lewis PW, Botchan MR. Isolation of the Cdc45/Mcm2-7/GINS (CMG) complex, a candidate for the eukaryotic DNA replication fork helicase. Proc Natl Acad Sci U S A 2006;103:10236–41.
6. Pacek M, Tutter AV, Kubota Y, Takisawa H, Walter JC. Localization of MCM2-7, Cdc45, and GINS to the site of DNA unwinding during eukaryotic DNA replication. Mol Cell 2006;21:581–7.
7. Chang YP, Wang G, Bermudez V, Hurwitz J, Chen XS. Crystal structure of the GINS complex and functional insights into its role in DNA replication. Proc Natl Acad Sci U S A 2007;104:12685–90.
8. De Falco M, Ferrari E, De Felice M, Rossi M, Hubscher U, Pisani FM. The human GINS complex binds to and specifically stimulates human DNA polymerase α-primase. EMBO Rep 2007;8:99–103.
9. Kamada K, Kubota Y, Arata T, Shindo Y, Hanaoka F. Structure of the human GINS complex and its assembly and functional interface in replication initiation. Nat Struct Mol Biol 2007;14:388–96.
10. Kubota Y, Takase Y, Komori Y, et al. A novel ring-like complex of *Xenopus* proteins essential for the initiation of DNA replication. Genes Dev 2003;17:1141–52.
11. Barkley LR, Song IY, Zou Y, Vaziri C. Reduced expression of GINS complex members induces hallmarks of pre-malignancy in primary untransformed human cells. Cell Cycle 2009;8:1577–88.
12. Ueno M, Itoh M, Kong L, Sugihara K, Asano M, Takakura N. PSF1 is essential for early embryogenesis in mice. Mol Cell Biol 2005;25:10528–32.
13. Han Y, Ueno M, Nagahama Y, Takakura N. Identification and characterization of stem cell-specific transcription of PSF1 in spermatogenesis. Biochem Biophys Res Commun 2009;380:609–13.
14. Ueno M, Itoh M, Sugihara K, Asano M, Takakura N. Both alleles of